Phytophthora infestans RXLR effectors target parallel steps in an immune signal transduction pathway

Ren, Yajuan; Armstrong, Miles; Qi, Yetong; McLellan, Hazel; Zhong, Cheng; Du, Bowen

Published in:
Plant Physiology

DOI:
10.1104/pp.18.00625

Publication date:
2019

Document Version
Peer reviewed version

Plant Physiology Preview. Published on June 19, 2019, as DOI:10.1104/pp.18.00625

Short title: Different effectors disable the same signal pathway.

Article Title: *Phytophthora infestans* RXLR effectors target parallel steps in an immune signal transduction pathway

Yajuan Ren[1, 2], Miles Armstrong[3,4], Yetong Qi[1, 2], Hazel McLellan[3], Cheng Zhong[1], Bowen Du[1, 2], Paul RJ Birch[3,4]§, Zhendong Tian[1, 2]§

[1]Key Laboratory of Potato Biology and Biotechnology, Ministry of Agriculture and Rural Affairs, Huazhong Agricultural University (HZAU), Wuhan 430070, People's Republic of China

[2]Key Laboratory of Horticultural Plant Biology (HZAU), Ministry of Education, Huazhong Agricultural University, Wuhan 430070, People's Republic of China

[3]Division of Plant Sciences, School of Life Science, University of Dundee (at James Hutton Institute), Errol Road, Invergowrie, Dundee DD2 5DA, UK

[4]Cell and Molecular Sciences, James Hutton Institute, Errol Road, Invergowrie, Dundee DD2 5DA, UK

§ **Authors for correspondence:** P.Birch@dundee.ac.uk; tianzhd@mail.hzau.edu.cn

One sentence summary: Two *P. infestans* effectors, PexRD2 and Pi22926, target two parallel MAP3K proteins in the same signal transduction pathway to promote *P. infestans* colonization.

Author contributions: Z.T and P.R.J.B conceived the research and designed the experiments. M.A and C.Z performed the original yeast-2-hybrid screen. Y.Q performed *N. benthamiana* transformations. Y.Q performed VIGS and cell death assay. B.D performed late blight resistance assay. R.Y performed most of the experiments. Y.R and Z.T performed data analysis and made figures. Y.R, M.H, P.R.J.B and Z.T. wrote the paper with contributions of all the authors. Z.T. and P.R.J.B secured funding.

Abstract

The potato (*Solanum tuberosum*) blight pathogen *Phytophthora infestans* delivers RXLR effector proteins into host cells to subvert plant immune responses and promote colonization. We show that transient expression and stable transgenic expression of the RXLR effector Pi22926 in *Nicotiana benthamiana* promotes leaf colonization by *P. infestans.* Pi22926 suppresses cell death triggered by co-expression of the *Cladosporium fulvum* avirulence protein Avr4 and the tomato (*Solanum lycopersicum*) resistance protein Cf4. Pi22926 interacts with a potato Mitogen Activated Protein Kinase Kinase Kinase, StMAP3Kβ2, in the nucleoplasm. Virus-induced gene silencing (VIGS) of the orthologue *NbMAP3Kβ2* in *N. benthamiana* enhances *P. infestans* colonization and attenuates Cf4/Avr4-induced cell death, indicating that this host protein is a positive regulator of immunity. Cell death induced by Cf4/Avr4 is dependent on NbMAP3Kε and NbMAP3Kβ2, indicating that these MAP3Ks function in the same signalling pathway. VIGS of *NbMAP3Kβ2* does not compromise cell death triggered by overexpression of MAP3Kε. Similarly, VIGS of *NbMAP3Kε* does not attenuate cell death triggered by MAP3Kβ2, demonstrating that these MAP3K proteins function in parallel. In agreement, Pi22926 or another RXLR effector PexRD2 only suppress cell death triggered by expression of StMAP3Kβ2 or StMAP3Kε, respectively. Our data reveal that two *P. infestans* effectors, PexRD2 and Pi22926, promote *P. infestans* colonization by targeting MAP3K proteins that act in parallel in the same signal transduction pathway.

Key words: effector-triggered immunity; hypersensitive response; effector-triggered susceptibility; late blight; oomycete

Introduction

Plants have a two-layer surveillance system to respond to pathogens and mount defenses against attack (Jones and Dangl, 2006; Dodds and Rathjen, 2010). The first layer is initiated at the host cell surface by pattern recognition receptors (PRRs) that detect microbe-associated molecular patterns (MAMPs), such as bacterial flagellin, elongation factor EF-Tu, peptidoglycans and lipopolysaccharide (Couto and Zipfel, 2016). This detection system results in pattern-triggered immunity (PTI), accompanied by activation of mitogen activated protein kinase (MAPK) signalling cascades, production of reactive oxygen species (ROS), callose deposition in the cell wall and the induction of pathogenesis-related (PR) protein expression (Chisholm et al., 2006; Jones and Dangl, 2006). In turn, successful plant pathogens deliver a range of effector proteins that act in the apoplast or within plant cells to attenuate PTI. Our understanding of how effectors manipulate host targets to interfere with defense pathways and processes has been led by the studies of bacterial type III secreted effectors (Dou and Zhou, 2012; Block and Alfano, 2011; Deslandes and Rivas, 2012). More recently, the targets of effectors from filamentous plant pathogens such as fungi and oomycetes have been revealed (Toruño et al., 2016; Whisson et al 2016; Anderson et al., 2015). Plants possess resistance (R) proteins which perceive effectors or effector activities, leading to effector-triggered immunity (ETI). This causes rapid and localized programmed cell death (PCD), ROS production and prolonged MAPK activation (Jones and Dangl, 2006).

The MAPK cascade is a core module for signal transduction in response to extracellular stimuli in plants. MAPK pathways play important roles in activation of plant immune responses mediated by both PRR and R proteins (Pedley and Martin, 2005; Pitzschke et al., 2009). MAPK pathways generally include three protein kinases: MAP kinase kinase kinase (MAP3K), MAP kinase kinase (MAP2K) and MAP kinase (MAPK). The MAPK is phosphorylated by a MAP2K, which itself is phosphorylated by a MAP3K. In the *Arabidopsis thaliana* genome, there are at least 20 putative MAPKs, 10 MAP2Ks, and more than 80 MAP3Ks (Pitzschke et al., 2009).

MAP3Ks can be divided into a further 3 groups. These are the MEKK (MAPK/ERK kinase kinase)-like subgroup which function as MAP3Ks in plants and mainly participate in linear cascades and the ZIK-like and Raf-like groups, functional characterization of which largely comes from organisms other than plants (MAPK Group, 2002; Colcombet and Hirt, 2008). Only a limited number of MAP3Ks are associated with regulating plant immunity. For example, Arabidopsis MEKK1 is activated downstream of the PRR FLS2 which detects the bacterial MAMP flg22. Studies have shown that MEKK1 regulates MEKK1-MKK1/2-MPK4, which negatively regulates plant defense responses (Gao et al., 2008; Suarez-Rodriguez et al., 2007). More recently, the MAP3Ks MAPKKK3 and MAPKKK5, which are activated by receptor-like cytoplasmic kinase VII family members, are responsible for activating the MAPKs MPK3/MPK6 (Bi et al., 2018). Conversely, the MAP3K YODA, which promotes stomatal development, directly inhibits the MAPKKK3/MAPKKK5 activation of MPK3/MPK6, demonstrating the antagonism that exists between plant growth and immunity (Sun et al., 2018).

Nicotiana benthamiana MAP3K NPK1 is essential for regulating the resistance responses mediated by the R proteins N, Bs2, and Rx, and may play roles in one or more MAPK cascades (Jin et al., 2002). Tomato (*Solanum lycopersicum*) MAP3Kα is involved in two distinct MAPK cascades, either MEK2-SIPK or MEK1-NTF6, to regulate plant immunity (del Pozo et al., 2004). Tomato MAP3Kε activates the MEK2-SIPK/WIPK cascade to positively regulate defense (Melech-Bonfil and Sessa, 2010). Finally, the Arabidopsis Raf-like MAP3K EDR1 was found to negatively regulate plant immunity (Frye et al., 2001).

Oomycete pathogens, ranging from obligate biotrophs to necrotrophs, deploy a variety of apoplastic and intracellular effectors (Kamoun et al., 2015). The best studied intracellular effectors are the RXLR class, which contain a signal peptide followed by a conserved Arg-X-Leu-Arg (RXLR) motif. It has been reported that the RXLR peptide motif acts as a host-targeting signal for translocation into host plant cells to suppress plant immunity (Whisson et al., 2007; Dou et al., 2008). Recently,

delivery of RXLR effectors from the oomycete potato blight pathogen *Phytophthora infestans* into plant cells has been visualized, revealing that they are secreted via a non-canonical pathway (Wang et al., 2017; 2018a).

Since the bacterial type 3 effector HopAI1 was shown to suppress activation of MPK3 and MPK6 in Arabidopsis, a range of phytopathogen effectors have been implicated in targeting MAPK pathways (Bi and Zhou, 2017). RXLR effectors from *P. infestans* have been shown to suppress MAPK signaling cascades, or to interact with MAP3K components to interfere with immunity (Whisson et al., 2016). Three RXLRs, Pi13628/SFI5/PexRD27, Pi13959/SFI6 and Pi18215/SFI7/Avr3b are able to suppress flg22-triggered MAMP signaling at, or upstream of, the MAPK cascade in tomato (Zheng et al., 2014). The effector Pi11383/PexRD2 specifically targets the kinase domain of MAP3Kε, directly inhibiting its activity to perturb plant defense responses (King et al., 2014). Recently, Murphy et al. (2018) reported that the effector Pi17316 interacts with the host MAP3K, StVIK, which acts as a susceptibility (S) factor to enhance *P. infestans* colonization.

In this study we show that the *P. infestans* effector PITG_22926 (Pi22926) targets the potato (*Solanum tuberosum*) MAP3K, StMAP3Kβ2, a positive regulator of immunity, to facilitate disease. Transient or stable expression of the RXLR effector Pi22926 in the model host *N. benthamiana* promotes the growth of *P. infestans* and specifically suppresses cell death induced by co-expression of the tomato resistance protein Cf4 with the *Cladosporium fulvum* avirulence protein Avr4. Pi22926 interacts with the kinase domain of StMAP3Kβ2 in a yeast two-hybrid (Y2H) library screen and *in planta*. Virus-induced gene silencing (VIGS) of *MAP3Kβ2* in *N. benthamiana* enhanced *P. infestans* colonization and attenuated Cf4/Avr4-induced cell death, indicating that it is a positive regulator of plant immunity. Overexpression of StMAP3Kβ2 or its kinase domain induced cell death in *N. benthamiana* which is suppressed by Pi22926. Epistasis experiments revealed that StMAP3Kβ2 acts in parallel to StMAP3Kε, and upstream of MEK2. Our results reveal a *P. infestans* effector protein that interacts with host StMAP3Kβ2 to target the same signaling

pathway as PexRD2 for immune suppression.

Results and Discussion

The RXLR effector Pi22926 promotes *P. infestans* colonization

The RXLR effector gene *PITG_22926* (*Pi22926*) was shown previously to be up-regulated at 2 and 3 days post *P. infestans* infection of potato leaves in both genotype T30-4 and genotype 13_A2 (Haas et al., 2009; Cooke et al., 2012), and more recently in diverse potato genotypes in China and during tuber infection (Yin et al., 2017; Ah-Fong et al., 2017). Here, we confirmed that *Pi22926* is also up-regulated in *P. infestans* isolate HB09-14-2 at 24, 48 and 72 h post-inoculation of a Chinese potato variety ‘E-potato-3’ (Supplemental Figure S1). The time course suggests that Pi22926 contributes to the biotrophic phase of infection, similar to other PiRXLR effectors (Whisson et al., 2016). Recently, Pi22926 has been shown to be secreted from *P. infestans* haustoria and delivered into host cells to accumulate in the nucleus (Wang et al., 2018a), where it enhances *P. infestans* colonization of *N. benthaminana* (Wang et al., 2018b). We confirmed that the disease lesion diameters on the half leaves transiently expressing GFP-Pi22926 (the signal peptide was deleted) were significantly larger compared to the GFP control six days post–inoculation (Supplemental Figure S2). The GFP-Pi22926 fusion protein was intact when transiently expressed in *N. benthamiana* leaves (Supplemental Figure S3A).

To explore this phenomenon further, transgenic *N. benthamiana* plants were made for stable expression of GFP-Pi22926. *GFP-Pi22926* expression was detected in 4 transgenic lines (Supplemental Figure S4). All 4 lines showed growth and morphology similar to wild type and 2 lines were thus taken forward for detailed study. Leaves from transgenic plants were infected with *P. infestans* and were found to sustain significantly larger *P. infestans* lesions compared to wild-type control plants (Figure 1A, B). The GFP-Pi22926 fusion protein was intact in transgenic *N. benthamiana* leaves (Supplemental Figure S3C). These results reveal that GFP-Pi22926 activity within host cells is beneficial to *P. infestans* colonization.

Pi22926 specifically suppresses Avr4/Cf4 and AvrPto/Pto triggered cell death

Co-expression of the *C. fulvum* avirulence protein Avr4 and the tomato resistance protein Cf4, or the *Pseudomonas syringae* avirulence protein AvrPto and corresponding tomato resistance protein component Pto, triggers cell death in *N. benthamiana via* activation of a common signaling pathway. The PiRXLR effector PexRD2 was previously shown to specifically suppress Avr4/Cf4 and Avrpto/Pto triggered cell death (King et al., 2014), and we confirmed these results as a positive control in this study (Figure 2). In addition, our results reveal that Avr4/Cf4 and AvrPto/Pto triggered cell death were significantly attenuated by co-expression with Pi22926 compared with the empty vector control (Figure 2A, 2B). We also tested whether Pi22926 is able to suppress cell death trigged by the *P. infestans* avirulence protein ($Avr3a^{KI}$) and resistance protein R3a pairs (Armstrong et al., 2005), or potato virus X (PVX) coat protein (PVX-CP) and PVX resistance protein (RX) pairs (Moffett et al., 2002), and by *P. infestans* MAMP INF1 (Kamoun et al., 1998). No change to the mean percentage of cell death mediated by these elicitors was observed in the presence of Pi22926 (Figure 2B), indicating that they are independent of the signal transduction cascade(s) manipulated by Pi22926 or PexRD2. These results indicate that Pi22926 and PexRD2 may suppress the same specific signalling pathway to promote disease.

Pi22926 specifically targets potato MAP3Kβ2

To identify possible host targets of Pi22926, a yeast-2-hybrid (Y2H) library composed of cDNA from potato plants infected with *P. infestans* (Bos et al., 2010) was screened with Pi22926 as a bait. The screen involved approximately 1.2×10^6 yeast co-transformants. Two yeast co-transformants growing on selection plates contained identical, partial sequences corresponding to a potato MAP3K (XP_006349414.1). Alignment of full-length amino acid sequences of MAP3Ks from potato, *N. benthamiana* and tomato showed that the potato interacting protein shares high identities with both a tomato protein (XP_004230523.1, identity: 94.59%) and a *N.*

benthamiana protein (Nbv6.1trP19888, identity: 82.64%). The tomato and potato proteins were reciprocal best Blast hits (RBBHs), and thus candidate orthologues, of NbMAP3Kβ2 (Supplemental Figure S5). The potato interacting protein was hence named StMAP3Kβ2. StMAP3Kβ2 contains a kinase domain at the C terminus (residues 402 to 653) (Supplemental Figure S5).

To investigate the specificity of the interaction between Pi22926 and StMAP3Kβ2, a pairwise Y2H assay was performed in which the full length StMAP3Kβ2, its active kinase domain (KD), and an inactive form in which the active site lysine in the ATP binding site (Lys 430) was substituted with an arginine, were used as prey clones against the bait Pi22926. In addition, two other RXLR effectors, PexRD2 (Pi11383) and Pi04089, were used as controls. PexRD2 targets another MAP3K in the cytoplasm, StMAP3Kε (King et al., 2014) and Pi04089 shows a similar nuclear localization to Pi22926 but interacts with the RNA binding protein StKRBP1 (Wang et al., 2015). While all yeast transformants grew on control +His plates, the interactions of Pi22926 with full length StMAP3Kβ2 or with its active KD were indicated by induction of β-galactosidase activity and growth on media lacking histidine (-His). The Pi04089 or PexRD2 combinations did not activate either reporter (Figure 3A, Supplemental Figure S6). In addition, whereas PexRD2 interacted with StMAP3Kε, no such interaction was observed between Pi22926 and StMAP3Kε (Supplemental Figure S6). Importantly, the mutant StMAP3Kβ2(KD)^{Lys430Arg} also failed to interact with Pi22926 (Figure 3A). This suggests that the intact active kinase domain of StMAP3Kβ2 is necessary and sufficient for the specific interaction with Pi22926.

To confirm that specific interactions also occur *in vivo*, a co-immunoprecipitation (co-IP) assay was performed by transiently co-expressing cMyc-StMAP3Kβ2(KD) or cMyc-StMAP3Kβ2(KD)^{Lys430Arg} with GFP-Pi22926, or with the GFP-Pi04089 control, following immunoprecipitation with GFP-TRAP_M beads. Intact GFP- or cMyc-labelled proteins were all stably expressed when corresponding constructs were transiently expressed in *N. benthamiana* leaves as indicated in the input samples. The cMyc-StMAP3Kβ2 (KD) was only pulled down in the presence of

Pi22926, but not with the Pi04089 control (Figure 3B). These results indicate that Pi22926 specifically interacts with StMAP3Kβ2 by its active kinase domain (KD) both in yeast and *in planta*.

Pi22926 interacts with StMAP3Kβ2 in the nucleoplasm

To investigate the subcellular localization of Pi22926 and StMAP3Kβ2, GFP was fused to their N or C terminus to form GFP-Pi22926 and StMAP3Kβ2-GFP and viewed following Agrobacterium-mediated expression in *N. benthamiana* using confocal microscopy. GFP-Pi22926 localized predominantly in the nucleus and nucleolus (Figure 4A). StMAP3Kβ2-GFP localized in the cytoplasm and showed weak fluorescence in the nucleoplasm, but was not observed in the nucleolus (Figure 4B). GFP-Pi22926 and StMAP3Kβ2-GFP were stable as fusion proteins *in planta* (Supplemental Figure S3A, B). When RFP-Pi22926 and StMAP3Kβ2-GFP were co-expressed by Agrobacterium-mediated expression in *N. benthamiana*, RFP-Pi22926 and StMAP3Kβ2-GFP were co-localized in the nucleus (Figure 4C), but StMAP3Kβ2-GFP still retained cytoplasmic fluorescence background. We thus investigated the interaction using bimolecular fluorescence complementation. When YN-Pi22926 and YC-StMAP3Kβ2 were co-expressed by Agrobacterium-mediated expression in *N. benthamiana,* reconstituted YFP fluorescence was observed only in the nucleoplasm (Figure 4D). By contrast, when YC-StMAP3Kβ2 was co-expressed with YN-Pi04089 (Wang et al., 2015), only weak background fluorescence was observed (Figure 4E). YN-Pi22926, YN-Pi04089 and YC-StMAP3Kβ2 were stable as fusion proteins *in planta* (Supplemental Figure S3D, E). This demonstrates that the interaction between these proteins occurs in the nucleoplasm, despite both showing some level of cytoplasmic localization. Further work is needed to look at substrates of StMAP3Kβ2 and where it phosphorylates them. Interestingly, StMAP3Kε and PexRD2 interacted in the cytoplasm, suggesting that there are alternative substrates for phosphorylation at that location that contribute to cell death (King et al., 2014).

Silencing of *NbMAP3Kβ2* promotes *P. infestans* colonization

To investigate the potential role of StMAP3Kβ2 in plant defense responses to *P. infestans*, VIGS was employed to knock-down the expression of *NbMAP3Kβ2* (orthologue of *StMAP3Kβ2*) in the model host plant *N. benthamiana*. We confirmed that GFP-Pi22926 is able to interact with the kinase domains of both StMAP3Kβ2 and NbMAP3Kβ2 in yeast and *in planta* (Supplemental Figure S7A, B). Two VIGS vectors containing independent portions of the *NbMAP3Kβ2* gene, TRV:NbMAP3Kβ2-5' and TRV:NbMAP3Kβ2-3', were generated to specifically knock down this gene in *N. benthamiana* (Supplemental Figure S8A). Transcript levels of the target gene in plants expressing each of the TRV:NbMAP3Kβ2 constructs was reduced by 70%-80%, but *NbMAP3Kε* transcript levels were unaltered (Supplemental Figure S8B). VIGS plants showed a developmentally normal phenotype when compared with the TRV:GFP control. TRV:NbMAP3Kβ2 and TRV-GFP plants were infected with *P. infestans* isolate 88069. Seven days post-inoculation (dpi), measurements of both *P. infestans* lesion diameter and sporangia production on TRV:GFP and TRV:NbMAP3Kβ2-5' and TRV:NbMAP3Kβ2-3'-expressing *N. benthamiana* plants showed that silencing of *NbMAP3Kβ2* significantly enhanced *P. infestans* colonization compared with the TRV:GFP control (Figure 5A, B, C). This indicates that NbMAP3Kβ2 is potentially a positive regulator of plant immunity.

Cell death induced by Avr4/Cf4 and AvrPto/Pto is dependent on MAP3Kβ2

As Pi22926 suppresses Cf4/Avr4 and Pto/AvrPto cell death, we hypothesised that MAP3Kβ2 may act in the signal transduction pathways leading to these cell death responses. To test that, TRV:NbMAP3Kβ2-5' and TRV:NbMAP3Kβ2-3' were used to silence *NbMAP3Kβ2* in *N. benthamiana* plants, and the leaves of VIGS plants were infiltrated with the *Agrobacterium tumefaciens* harboring effector/R protein pairs Avr4/Cf4 and AvrPto/Pto. As expected, similar to the silencing of *MAP3Kε* (specific silencing efficiency shown in Supplemental Figure S9), we observed that silencing of *NbMAP3Kβ2* significantly reduced the percentage of sites developing cell death

upon co-expression of Avr4/Cf4 or AvrPto/Pto, compared with the TRV:GFP empty vector control (Figure 6). However, silencing of *NbMAP3Kβ2* and *NbMAP3Kε* did not compromise INF1, Avr3a/R3a or RX/CP triggered cell death (Supplemental Figure S10), indicating that silencing of *NbMAP3Kβ2* specifically compromises Avr4/Cf4 or AvrPto/Pto triggered cell death. Taken together, our results suggest that NbMAP3Kβ2, like MAP3Kε (King et al., 2014), plays an essential role in the signaling pathway activated by Avr4/Cf4 or AvrPto/Pto.

Pi22926 suppresses cell death induced by expression of StMAP3Kβ2 and its kinase domain

Expression of the full length and kinase domain (KD) of some MAP3Ks in *N. benthamiana* induces cell death (Hashimoto et al., 2012). To determine whether overexpression of StMAP3Kβ2 is able to induce cell death, we used Agrobacterium to transiently express the full length StMAP3Kβ2, its active KD, or the inactive form $(KD)^{Lys430Arg}$ in *N. benthamiana* leaves. We observed that overexpression of StMAP3Kβ2 or its KD alone resulted in pathogen- and elicitor-independent cell death compared to the GFP control. In contrast, cell death was not observed in leaves expressing inactive $KD^{Lys430Arg}$, suggesting that an intact kinase catalytic domain is essential for StMAP3Kβ2 to trigger cell death (Figure 7A, C). As Pi22926 was shown to interact with StMAP3Kβ2 (Figure 3), this prompted us to test whether Pi22926 has any effect on the cell death induced by StMAP3Kβ2. We co-expressed GFP-Pi22926 with StMAP3Kβ2 or its KD in *N. benthamiana* using Agrobacterium-mediated expression. Seven days post-agroinfiltration, we observed that StMAP3Kβ2- and KD-induced cell death was significantly suppressed by co-expression with GFP-Pi22926 compared to the GFP control. This indicates that Pi22926 is a suppressor of cell death triggered by StMAP3Kβ2 (Figure 7B, D).

MEK2 and SIPK act downstream of StMAP3Kε and StMAP3Kβ2

To test whether StMAP3Kε and StMAP3Kβ2 share the same downstream signaling

cascade, VIGS constructs that silence *MEK1* and *MEK2* (encoding MAP2Ks), or constructs for silencing wound-induced protein kinase gene *WIPK,* salicylic acid-induced protein kinase gene *SIPK* or *NTF6* (MAPKs) were generated and used to silence corresponding genes in *N. benthamiana* plants. The efficiency of silencing was assessed by RT-qPCR analysis that measured the expression of each target gene in silenced plants relative to control TRV:GFP plants (Supplemental Figure S11). Typical cell death was observed on the leaves of TRV:GFP control plants when expressing intact KDs of StMAP3Kε and StMAP3Kβ2, but mutated KDs (as a negative control) did not induce cell death (Figure 8A). Intact KDs of StMAP3Kε and StMAP3Kβ2 were also able to induce cell death in both TRV: MEK1 and TRV:NTF6 VIGS plants (Figure 8A). However, silencing of *MEK2*, *WIPK* and *SIPK* significantly inhibited the cell death triggered by the expression of intact KDs of StMAP3Kε (Figure 8A, B). This result is in agreement with the tomato SlMAP3Kε which mediated a cell death signaling cascade involving the MAP2K MEK2 and the two MAPKs WIPK and SIPK rather than MEK1 or NTF6 (Melech-Bonfil and Sessa, 2010). Interestingly, although the cell death triggered by StMAP3Kβ2 needed MEK2 and SIPK, similar to StMAP3Kε, silencing WIPK did not abolish StMAP3Kβ2 triggered cell death (Figure 8A, C). This indicates that StMAP3Kε and StMAP3Kβ2 share the same signal transduction pathway but there is a difference downstream of MEK2.

Pi22926 suppresses StMAP3Kβ2-triggered cell death but does not suppress StMAP3Kε-triggered cell death

A previous study reported that the *P. infestans* RXLR effector PexRD2 suppresses cell death triggered by activity of the kinase domain of MAP3Kε (King et al., 2014). We show that Pi22926 suppresses StMAP3Kβ2(KD) triggered cell death, whereas the effectors PexRD2, Pi13959, Pi13628 and Pi18215 failed to do so (Figure 9A, B). To test whether Pi22926 suppresses StMAP3Kε-triggered cell death, Pi22926 and StMAP3Kε(KD) were transiently co-expressed in *N. benthamiana*. We found that Pi22926 cannot suppress StMAP3Kε(KD)-triggered cell death, whereas PexRD2

does (Figure 9C, D). These results indicate that StMAP3Kβ2 and StMAP3Kε likely act at the same level in the cell death signalling pathway.

StMAP3Kβ2 acts in parallel with StMAP3Kε in Cf4/AVR4 induction of cell death

Epistasis analysis of the functional relationships among NbMAP3Kβ, NbMAP3Kγ, and NbMAP3Kα suggested that these three MAP3Ks form a linear signalling pathway which proceeds from NbMAP3Kβ to NbMAP3Kγ to NbMAP3Kα to lead to cell death (Hashimoto et al., 2012). We have shown that NbMAP3Kβ2 and MAP3Kε are involved in the same signalling pathway in that they positively regulate Avr4/Cf4 and AvrPto/Pto signal transduction (Figure 6). The observation that Pi22926 or PexRD2 can only suppress cell death during transient co-expression with NbMAP3Kβ2 or MAP3Kε, respectively, suggests that MAP3Kε and NbMAP3Kβ2 may function at the same level in the signal transduction pathway.

To confirm this, we silenced each gene using VIGS in *N. benthamiana.* Silencing of *NbMAP3Kβ2* did not significantly (ANOVA, $p<0.001$) suppress MAP3Kε triggered cell death (Figure 9E) compared to the TRV:GFP control. VIGS of *NbMAP3Kε* did not suppress the cell death induced by transient expression of NbMAP3Kβ2 (Figure 9F). Taken together, these results confirm that MAP3Kε and MAP3Kβ2 act in parallel in the same signalling pathway in Cf4/AVR4 cell death induction.

Perception of the *P. infestans* MAMP INF1 triggers a MAPK pathway that is independent of MAP3Kε and MAP3Kβ2, and is thus not suppressed by the effectors PexRD2 (King et al., 2014) or Pi22926. In contrast, as yet unidentified receptor(s) activated by unknown *P. infestans* elicitor(s) trigger a MAPK cascade that includes StMAP3Kε and StMAP3Kβ2, resulting in activation of MAP2K MEK2 and finally SIPK/WIPK (Figure 10), ultimately leading to cell death. The importance of the StMAP3Kε/StMAP3Kβ2-MEK2-SIPK/WIPK pathway in immunity to *P. infestans* is highlighted by the fact that these two RXLR effectors from distinct MCL cluster families (Haas et al., 2009), PexRD2 (RXLRfam6) and Pi22926 (RXLRfam52), which

act to suppress parallel regulatory steps (Figure 10).

Future work will reveal whether other *P. infestans* RXLRs target additional members of this MAPK cascade to redundantly suppress this immune pathway, or indeed may target additional MAPK signal transduction pathways associated with immune responses. In the large-scale effector yeast-2-hybrid screens of Mukhtar et al. (2011) and Weβling et al. (2014) MAPK signaling components did not emerge as 'hubs' that are targeted by effectors from different pathogens. Nevertheless, type III effectors from bacterial plant pathogens, such as hopAI1 from *P. syringae*, which targets MPK3 and MPK6, can also directly inactivate MAPK cascade components that positively regulate immunity. Moreover, the *P. syringae* effector AvrB targets MPK4 to promote its activity as a negative regulator of immunity (Cui et al., 2010), and the *P. infestans* effector Pi17316 targets the susceptibility factor VIK, also to exploit its role as a negative immune regulator (Murphy et al., 2018). Thus bacterial and oomycete effectors directly target both positive and negative regulators of immunity within MAPK cascades.

In conclusion, this study emphasizes the power of effectors as probes to dissect and understand the regulation of plant immune signaling pathways. However, the PRR that perceives a *P. infestans* molecule to initiate the StMAP3Kε/StMAP3Kβ2-MEK2-SIPK/WIPK pathway is unknown, highlighting the need to more deeply invest in identifying cell surface receptors and the pathogen ligands that they detect to activate defence.

Materials and methods

Plant materials

Nicotiana benthamiana plants were grown in individual plots in the greenhouse with 16 h days at 22 °C and 8 h nights at 18 °C. Approximately 4–5-week-old *N. benthamiana* were used for experiments. A Chinese potato (*Solanum tuberosum*)

variety ‘E-potato-3’ was used for *Pi22926* expression tests. *In vitro* cultured plantlets were grown in the greenhouse as above. Leaves from 8 weeks old plants were used for *Phytophthora infestans* inoculation.

Plasmid construction

The RXLR effectors Pi22926 and Pi04089 were cloned without signal peptides from genomic DNA of *P. infestans* isolate T30-4 in a two-step PCR to add flanking attB sites to the coding sequences. The potato StMAP3Kβ2 coding sequence was amplified from the original yeast-2-hybrid (Y2H) prey library using the same strategy. The Y2H library was the same as that used by McLellan et al. (2013) and Yang et al. (2016).

The PCR products were purified and cloned into pDONR221 (Invitrogen) to generate entry clones via BP reactions. The effector entry clones were transferred into pB7WGF2 (for N-terminal eGFP fusion), pK7WGR2 (for N-terminal RFP fusion), and pDEST32 (for Y2H, Invitrogen). The StMAP3Kβ2 and StMAP3Kβ2 (KD) were recombined with pK7FWG2 (for C-terminal eGFP fusion) and pDEST22 (for Y2H; Invitrogen). For N-terminal cMyc tagging, pH7LIC was generated using the ClonExpress Entry One Step Cloning Kit (Vazyme, Vazyme Biotech Co, Ltd, China). For splitYFP constructs, Pi04089 and Pi22926 were recombined with pCL112 (for N-terminal YN- fusion). StMAP3Kβ2 was recombined with pCL113 (for N-terminal YC- fusion).

Site-directed mutation of Lys430Arg in the StMAP3Kβ2 kinase catalytic domain was introduced using the Mut Express II Fast Mutagenesis Kit (Vazyme).The entry clone containing the mutated form of StMAP3Kβ2 was recombined into pDEST22 for Y2H and pK7FWG2 for *in planta* assays. For N-terminal tagging with the cMyc epitope, pH7LIC was generated for Co-immunoprecipitation analyses. Primer sequences used for PCR amplification and vector construction are shown in Supplemental Table S1.

***N. benthamiana* transformation**

Agrobacterium tumefaciens containing overexpression vector pB7WGF2 was used to transform leaf discs of *N. benthamiana*. Positive lines were first screened on differential medium (MS + 2 mg/L 6-BA + 0.2 mg/L NAA +1.5 mg/L Bialaphos (sodium salt) + 400 mg/L Cef + 30 g/L sucrose, pH 5.7) and then transferred to root generation medium (MS + 0.36 mg/L Bialaphos (sodium salt) + 200 mg/L Cef + 0.1 mg/L NAA + 30 g/L sucrose, pH 5.7). The positive lines were confirmed by semi-quantitative RT-PCR. Primers are shown in Supplemental Table S1).

Agro-infiltration and *P. infestans* infection assay

A. tumefaciens strain GV3101 harboring plasmid constructs were grown overnight in YEB medium with appropriate antibiotics at 28 °C at 200 rpm. The bacteria was pelleted, resuspended in sterile 10 mM MES; 10 mM $MgCl_2$ and 200 µM acetosyringone, and subsequently adjusted to the appropriate final OD_{600} before pressure infiltration into *N. benthamiana* leaves (generally 0.1 for infection assays, 0.3–0.5 for cell death and 0.5–1.0 for western blot and co-immunoprecipitation assays). For co-expression, agrobacteria cultures containing the appropriate vector constructs were mixed at a 1:1 ratio before infiltration. Each assay consisted of at least 8 plants inoculated on 3–4 leaves.

P. infestans strain 88069 was grown on Rye Sucrose Agar (RSA) plates at 18 °C in the dark for 14 days. Sporangia were harvested from RSA plates by adding 3 mL H_2O to the plates and zoospores were collected after one hour of incubation at 4 °C. Droplets (10 µL) of a solution of 100, 000 zoospores per mL were applied onto the abaxial side of detached *N. benthamiana* leaves and incubated for several days on wet paper towels in 100% relative humidity. *Agrobacterium tumefaciens* Transient Assays (ATTA) in combination with *P. infestans* infection were carried out as described (McLellan et al., 2013). For VIGS, the mean lesion diameter was measured at 7 dpi and compared to the GFP control. Sporangia counts were performed on 10 dpi leaves from VIGSed plants which had been washed in 5 ml H_2O and vortexed to release sporangia. The number of sporangia recovered from each leaf was counted using a hemocytometer.

Yeast-two-hybrid

A Y2H screen with pDEST32-Pi22926 was performed as described (McLellan et al., 2013) using the ProQuest two-hybrid system (Invitrogen). The coding sequence of StMAP3Kβ2, StMAP3Kβ2(KD) and StMAP3Kβ2(KD)^{Lys430Arg} were recombined into pDEST22 and re-tested with pDEST32-Pi22926 (pDEST32-Pi04089 as negative control) in pairwise interactions. The transformants were selected using SD/-Leu-Trp-His selective medium and X-gal assay to detect the reporter gene activation.

Co-immunoprecipitation

Leaves of 5-week-old *N. benthamiana* were respectively agro-infiltrated with GFP-Pi22926 (GFP-Pi040489 as a negative control), cMyc-tagged StMAP3Kβ2(KD) and cMyc-tagged StMAP3Kβ2(KD)^{Lys430Arg}. Two days after agro-infiltration, four leaf discs (9 mm in diameter) were harvested and proteins were extracted. GFP tagged Pi22926/ Pi04089 fusions were immunoprecipitated using GFP-Trap-M magnetic beads (MBL Biological Laboratories Co., Lid. URL).The resulting samples were separated by SDS-PAGE and western blotted. Immunoprecipitated GFP fusions and co-immunoprecipitated c-Myc fusions were detected using appropriate antisera (Sungene Biotech, China).

Confocal microscopy

A. tumefaciens（OD_{600}=0.03–0.1）containing target protein fusions were infiltrated into leaves of 4-week old *N. benthamiana* plants. *N. benthamiana* leaf cells expressing fluorescent protein fusions were imaged no later than 2 days after agroinfiltration using a CLSM (Leica TCS-SPE, Germany) confocal microscope. GFP was excited with 488 nm from an argon laser and its emissions were detected between 500 and 530 nm. mRFP was excited with 561 nm and its emissions were detected between 600 and 630 nm. Split-YFP was excited using 514 nm from an argon laser with emissions detected from 530 to 575 nm. Images were collected from leaf cells expressing low levels of the fluorescence to minimize artefacts of ectopic protein

expression.

Virus Induced Gene Silencing

Plasmids pTRV1 and pTRV2 were used for VIGS (Liu et al., 2002; Ekengren et al., 2003). Constructs pTRV2:NbSIPK, pTRV2:NbWIPK, pTRV2:NbMEK1, pTRV2: NbMEK2 and pTRV2: NbNTF6 were generated using the same gene fragments based on the construct information previously published (Asai et al., 2008； Melech-Bonfil and Sessa, 2010). pTRV2: NbMAPKKKε-5' and pTRV2: NbMAPKKKε-3' used in this study have been described (Melech-Bonfil and Sessa, 2010). For pTRV2: NbMAP3kβ2, 300 bp PCR fragments were cloned from *N. benthamiana* cDNA and inserted to pBinary Tobacco Rattle Virus (TRV) vectors (Liu et al., 2002) between *Bam*H I and *Eco*R I sites in the antisense orientation. A TRV construct expressing GFP described previously was used as a control (McLellan et al., 2013). *A. tumefaciens* strains harboring pTRV2 vectors combined with that harboring the pTRV1 vector were mixed at a 1:1 ratio and adjusted to OD_{600}=0.5. The co-cultures were then infiltrated into two primary leaves of a plant at the 4-leaf-stage. Plants were used for assays or to check gene silencing levels by RT-qPCR 2-3 weeks later. The primers and constructs used in this study are shown in Supplemental Table S1.

Gene expression assay

Three leaf discs (9 mm in diameter) were collected from *N*. *benthamiana* VIGS plants to extract total RNA using the PLANTpure Plant RNA Kit (Aidlab Biotechnologies, China). The first strand cDNA was synthesized from 2 μg of RNA using the TRUEscript 1st Strand cDNA Synthesis Kit With gDNA Eraser (Aidlab Biotechnologies, China). RT-qPCR reactions were performed using Power SYBR Green (Bio-Rad, USA). The *N*. *benthamiana* gene *EF1*α was used as a reference control. Primer pairs were designed outside the region of the cDNA targeted for silencing. The primers are shown in Supplemental Table S1. Gene expression levels were calculated by a comparative ΔΔCt method as described by Bio-Rad instruction.

Statistical analyses

All data and statistical analysis were carried out using one-way ANOVA and pairwise or multiple comparisons in Graphpad Prism 6.0 software (GraphPad Prism Software Inc., San Diego, CA, USA). All values and error bars presented are means and standard deviation (SD) or standard error (SE) of three or more experimental replicates.

Accession Numbers

Sequence data from this article can be found in the GenBank and website under the following accession numbers. *P. infestans* PITG_22926 (EEY57148), PexRD2 (EEY62542); potato StMAP3Kβ2 (XP_006360216.1), StMAP3Kε (KJ504180); Tomato SlMAPKKKβ1 (XP_010323778.1), SlMAPKKKβ2 (XP_004230523.1). *N. benthamiana* NbMAPKKKβ (BAM36967.1), NbMAP3Kβ2 (Nbv6.1trP19888, http://benthgenome.qut.edu.au/), NbMAP3Kε (ADK36643 and BAM36969).

Supplemental Materials

Supplemental Figure S1. Expression of *Pi22926* in a *P. infestans* infection time course on potato plants.

Supplemental Figure S2. The RXLR effector Pi22926 enhances *P. infestans* colonization of *N. benthamiana* leaves following Agrobacterium-mediated expression compared to a GFP control.

Supplemental Figure S3. Stability of the target proteins labeled by different tags in *N. benthamiana*.

Supplemental Figure S4. Expression of *Pi22926* in stable transgenic *N.*

benthamiana lines tested by RT-PCR.

Supplemental Figure S5. Alignment of MAP3Kβ2s from tomato, potato and *N. bethamiana.*

Supplemental Figure S6. Pi22926 does not interact with StMAP3Kε(KD) in yeast.

Supplemental Figure S7. Pi22926 interacts with NbMAP3Kβ2(KD) in yeast and *in planta*.

Supplemental Figure S8. NbMAP3Kβ2 constructs and silencing efficiency.

Supplemental Figure S9. Silencing efficiency of *NbMAP3Kε*.

Supplemental Figure S10. Cell death responses in *MAP3Kβ2* silenced *N. benthamiana* plants.

Supplemental Figure S11. *MEK1*, *MEK2*, *SIPK*, *WIPK* and *NTF6* silencing efficiency in *N. benthamiana* plants.

Supplemental Table S1. Primers and constructs used in this study.

Acknowledgements

We are grateful for financial support from the National Natural Science Foundation of China (Grants No. 31761143007, 31471550) and the Fundamental Research Funds for the Central Universities of China (Grant No. 2662017PY069), for funding ZT's lab, the Biotechnology and Biological Sciences Research Council (BBSRC) (grants BB/G015244/1, BB/K018183/1, BB/L026880/1) for PRJB, HM, MA, and The Scottish Government Rural and Environment Science and Analytical Services Division (RESAS) for funding PRJB.

Figure Legends

Figure 1. The RXLR effector Pi22926 enhances *P. infestans* colonization of *N. benthamiana* leaves. (A) Representative images taken under UV light at 5 days after inoculation show that transgenic lines overexpressing GFP-Pi22926 enhance pathogen colonization compared to the untransformed *N. benthamiana* control. Scale bar represents 1 cm. (B) Graph shows a significant increase in *P. infestans* lesions in transgenic lines overexpressing GFP-Pi22926 compared to wild type *N. benthamiana* control (ANOVA, $p<0.001$, 3 reps, n=120). Lowercase letters on graphs denote statistically significant groups. Error bars represent ± SE.

Figure 2. Pi22926 specifically suppresses Avr4/Cf4 and AvrPto/Pto induced cell death. (A) Representative leaf image taken under UV light at 5 days showing Avr4/Cf4 and AvrPto/Pto cell death with EV, Pi22926 and PexRD2 positive control. (B) Graph showing Pi22926 and PexRD2 expression lead to a significant decrease ($p<0.001$, 3 reps, n=94) in cell death percentage trigged by Avr4/Cf4 and AvrPto/Pto. Lowercase letters on graphs denote statistically significant groups by one-way ANOVA, with pairwise comparisons performed with the Holm-Sidak method. Error bars represent ± SE.

Figure 3. Pi22926 interacts with the kinase domain of StMAP3Kβ2 in Y2H and immunoprecipitation assays. (A) Yeast co-expressing Pi22926 with StMAP3Kβ2 and its kinase domain grow on –histidine (-HIS) medium and had β-galactosidase (β-gal) activity, wheareas those co-expressed with the inactive mutant kinase domain StMAP3Kβ2(KD)^{Lys430Arg} or the control Pi04089 did not. (B) Co-immunoprecipitation from leaf extracts using GFP-trap (GFP IP) confirmed that cMyc tagged StMAP3Kβ2 KD specifically interacted with GFP-Pi22926 and not with Pi04089. Expression of constructs is indicated by +. Protein size markers are indicated in KDa, and protein loading is indicated by Coomassie brilliant blue (CBB) staining.

Figure 4. Pi22926 interacts with StMAP3Kβ2 in nucleoplasm. (A) Confocal images show that GFP-Pi22926 is localized in the nucleoplasm and nucleolus. (B)

StMAP3Kβ2-GFP is localized in the cytoplasm and nucleoplasm. For images of StMAP3Kβ2-GFP, the left one is a Z-stack, whereas the right one with higher magnification is a single optical section from the stack. (C) Images show transient co-expression of StMAP3Kβ2-GFP with RFP-Pi22926. (D) Images show transient co-expression of YC-StMAP3Kβ2 with YN-Pi22926. Inset image is a nucleus at higher magnification. (E) Images show transient co-expression of YC-StMAP3Kβ2 with YN-Pi04089. Scale bars represent 10 μm. OD_{600} of Agrobacteria suspension for GFP and RFP constructs is 0.1 and 0.03 for split YFP.

Figure 5. Silencing of *NbMAP3Kβ2* enhances *P. infestans* leaf colonization. (A) Images taken at 7 days after sporangia inoculation indicate more pathogen colonization on TRV:NbMAP3Kβ2 plants compared to the TRV:GFP control. Scale bar represents 1 cm. (B) Graph shows a significant increase (ANOVA, $p<0.001$, 3 reps, n=120) in *P. infestans* lesion diameter in plants expressing TRV:NbMAP3Kβ2-3' and TRV:NbMAP3Kβ2-5', compared with a TRV-GFP control. (C) Graph shows an increase in the average numbers of sporangia mL^{-1} collected from infected leaves expressing TRV:NbMAP3Kβ2-3' and TRV:NbMAP3Kβ2-5', compared with a TRV:GFP control (ANOVA, $p<0.001$, 3 reps, n=120). Lowercase letters on graphs denote statistically significant groups. Error bars represent ± SE.

Figure 6. Cell death induced by Avr4/Cf4 and Avrpto/Pto is dependent on MAP3Kε and NbMAP3Kβ2. (A) Graph showing a significant suppression of cell death (ANOVA, $p<0.001$, 3 reps, n=72) induced by Avr4/Cf4 in *NbMAP3Kβ2* silenced plants, and in positive control *NbMAP3Kε* silenced plants, compared to TRV2:GFP control. (B) Graph showing a significant decrease of cell death (ANOVA, $p<0.001$, 3 reps, n=72) triggered by Avrpto/Pto in *NbMAP3Kβ2* silenced plants, and positive control *NbMAP3Kε* silenced plants, compared to TRV2:GFP control. Error bars represent ± SE. Cell death numbers were counted at 6 days. Stars indicate significant difference to the TRV:GFP control.

Figure 7. Overexpression of StMAP3Kβ2 or its kinase domain induces cell death that is suppressed by Pi22926. (A) Images taken under UV light at 7 days after inoculation showing that transient overexpression of StMAP3Kβ2 and its kinase domain induce cell death in *N. benthamiana* whereas no cell death was triggered by the expression of the inactive mutant StMAP3Kβ2 (KD)^{Lys430Arg} or the empty vector control. (B) The cell death trigged by StMAP3Kβ2 and its active kinase domain is suppressed by co-expression with Pi22926, but not EV control. Images taken under UV light at 7 days. (C) Graph shows a significant increase in percentage of cell death compared to EV control and inactive mutant KD (ANOVA, $p<0.001$, 3 reps, n=72). (D) Graph shows that transient overexpression of Pi22926 can significantly suppress the cell death (ANOVA, $p<0.001$, 3 reps, n=72) induced by StMAP3Kβ2 and its active KD compared to EV control. Lowercase letters on graphs denote statistically significant groups. Error bars represent ± SE.

Figure 8. MEK2 and SIPK act downstream of StMAP3Kβ2. (A) *N. benthamiana* plants were infected with TRV:GFP only or were silenced for the indicated MAP2Ks (*MEK1* or *MEK2*) and MAPK (*SIPK, WIPK* or *NTF6*) genes. StMAP3Kβ2 kinase domain (KD) or inactive (KD mutant) were expressed in the leaves to measure cell death. Photos were taken under UV light at 7 days. (B) and (C) Graph showing a significant suppression of cell death trigged by StMAP3Kε(KD) or StMAP3Kβ2(KD) in TRV2:MEK2 and TRV2:SIPK plants compared to the TRV2:GFP control (ANOVA, $p<0.001$, 3 reps, $n\geq155$). Error bars represent ± SE.

Figure 9. Pi22926 suppresses cell death trigged by StMAP3Kβ2 whereas PexRD2 suppresses StMAP3Kε-induced cell death. (A) and (C) Images showing StMAP3Kβ2 (KD) and StMAP3Kε(KD) cell death at 7 days, following co-expression with indicated effectors. (B) and (D) Graphs showing percentage of inoculation sites

developing cell death at 7 days after co-expression of StMAP3Kβ2(KD) or StMAP3Kε(KD) with indicated effectors. A significant decrease of cell death percentage was observed when Pi22926 was co-expressed with StMAP3Kβ2(KD) or when PexRD2 was co-expressed with StMAP3Kε(KD), compared to co-expression with other effectors and the EV control (ANOVA, $p<0.001$, 4 reps, n=73). Lowercase letters on graphs denote statistically significant groups. Error bars represent ± SE. (E) Graph shows no significant decrease in mean percentage of cell death induced by StMAP3Kε in TRV2:NbMAP3Kβ2-3' and TRV2:NbMAP3Kβ2-5' plants compared to the TRV2-GFP control (7 days) (ANOVA, $p<0.001$, 4 reps, n=92) and (F) Graph shows that VIGS of MAP3Kε by TRV2:NbMAP3Kε-3' and TRV2-NbMAP3Kε-5' had no significant effect on StMAP3Kβ2-induced cell death compared to the TRV:GFP control (7 days). (ANOVA, $p<0.001$, 4 reps, n=132). Error bars represent ± SE.

Figure 10. Model of how PexRD2 and Pi22926 suppress two parallel MAPK signalling pathways triggered by Avr4/Cf4 or AvrPto/Pto. Schematic diagram illustrating *P. infestans* delivering PexRD2 and Pi22926 inside the host cell during infection. The cell death following recognition of the *C. fulvum* effector Avr4 by Cf4 and the *P. syringe* effector AvrPto mediated by Pto/Prf are dependent on MAPKKKε or MAP3Kβ2 is suppressed respectively by the presence of PexRD2 or Pi22926. PexRD2 or Pi22926 specifically interact with MAPKKKε or MAP3Kβ2 respectively. *In planta*, MAPKKKε and MAP3Kβ2 confer enhanced resistance against *P. infestans* likely due to recognition of an unidentified PAMP by a PRR or recognition of an effector/avirulence protein (AVR) by an R protein as proposed by King et al. (2014).

References

Ah Fong AMV, Kim KS, Judelson HS (2017) RNA-seq of life stages of the oomycete *Phytophthora infestans* reveals dynamic changes in metabolic, signal

transduction, and pathogenesis genes and a major role for calcium signaling in development. *BMC Genomics* 18: 198.

Anderson RG, Deb D, Fedkenheuer K, McDowell JM (2015). Recent Progress in RXLR Effector Research. *Mol Plant Microbe Interact* 28**,** 1063-1072.

Armstrong MR, Whisson SC, Pritchard L, Bos JI, Venter E, Avrova AO, Rehmany AP, Böhme U, Brooks K, Cherevach I, Hamlin N, White B, Fraser A, Lord A, Quail MA, Churcher C, Hall N, Berriman M, Huang S, Kamoun S, Beynon JL, Birch PR (2005) An ancestral oomycete locus contains late blight avirulence gene *Avr3a*, encoding a protein that is recognized in the host cytoplasm. *Proc Natl Acad Sci USA* 102: 7766-7771.

Asai S, Ohta K, Yoshioka H (2008) MAPK signaling regulates nitric oxide and NADPH oxidase-dependent oxidative bursts in *Nicotiana benthamiana*. *Plant Cell* 20: 1390-406.

Bi G, Zhou JM (2017) MAP kinase signaling pathways: a hub of plant-microbe interactions. *Cell Host and Microbe* 21: 270-273.

Bi G, Zhou Z, Wang W, Li L, Rao S, Wu Y, Zhang X, Menke FLH, Chen S, Zhou J-M (2018) Receptor-like cytoplasmic kinases directly link pattern recognition receptors to the activation of mitogen-activated protein kinase cascades. *Plant Cell* 30: 1543-1561.

Block A, Alfano JR (2011) Plant targets for *Pseudomonas syringae* type III effectors: virulence targets or guarded decoys? *Curr Opin Microbiol*. 14: 39-46.

Bos JI, Armstrong MR, Gilroy EM, Boevink PC, Hein I, Taylor RM, Tian Z, Engelhardt S, Vetukuri RR, Harrower B, Dixelius C, Bryan G, Sadanandom A, Whisson SC, Kamoun S, Birch PR (2010) *Phytophthora infestans* effector AVR3a is essential for virulence and manipulates plant immunity by stabilizing host E3 ligase CMPG1. *Proc Natl Acad Sci USA* 107: 9909-9914.

Chisholm ST, Coaker G, Day B, Staskawicz BJ (2006) Host–microbe interactions:

684 shaping the evolution of the plant immune response. *Cell* 124: 803-814.

685 Colcombet J, Hirt H (2008) Arabidopsis MAPKs: a complex signalling network
686 involved in multiple biological processes. *Biochemical J*. 413: 217-226.

687 Cooke DE, Cano LM, Raffaele S, Bain RA, Cooke LR, Etherington GJ, Deahl KL,
688 Farrer RA, Gilroy EM, Goss EM, Grünwald NJ, Hein I, MacLean D, McNicol JW,
689 Randall E, Oliva RF, Pel MA, Shaw DS, Squires JN, Taylor MC, Vleeshouwers
690 VG, Birch PR, Lees AK, Kamoun S (2012) Genome analyses of an aggressive
691 and invasive lineage of the Irish potato famine pathogen. *PLoS Pathog*. 8:
692 e1002940.

693 Couto D, Zipfel C (2016) Regulation of pattern recognition receptor signalling in
694 plants. *Nat Rev Immunol*. 16: 537-552.

695 Cui H, Wang Y, Xue L, Chu J, Yan C, Fu J, Chen M, Innes RW, Zhou JM (2010)
696 *Pseudomonas syringae* effector protein AvrB perturbs Arabidopsis hormone
697 signalling by activating MAP kinase 4. *Cell Host Microbe* 7: 164-175.

698 del Pozo O, Pedley KF, Martin GB (2004) MAPKKKalpha is a positive regulator of
699 cell death associated with both plant immunity and disease. *EMBO J*. 23:
700 3072-3082.

701 Deslandes L, Rivas S (2012) Catch me if you can: bacterial effectors and plant
702 targets. *Trends Plant Sci.* 17: 644-655.

703 Dodds PN, Rathjen JP (2010) Plant immunity: Towards an integrated view of
704 plant-pathogen interactions. *Nat Rev Genet*. 11: 539-548.

705 Dou D, Kale SD, Wang X, Jiang RH, Bruce NA, Arredondo FD, Zhang X, Tyler BM.
706 (2008) RXLR-mediated entry of *Phytophthora sojae* effector Avr1b into soybean
707 cells does not require pathogen-encoded machinery. *Plant Cell* 20: 1930-1947.

708 Dou D, Zhou JM (2012) Phytopathogen effectors subverting host immunity: different
709 foes, similar battleground. *Cell Host Microbe* 12: 484-495.

710 Ekengren SK, Liu Y, Schiff M, Dinesh-Kumar SP, Martin GB (2003) Two MAPK

711 cascades, NPR1, and TGA transcription factors play a role in Pto-mediated
712 disease resistance in tomato. *Plant J*. 36: 905-917.

713 Frye CA, Tang D, Innes RW (2001) Negative regulation of defense responses in
714 plants by a conserved MAPKK kinase. *Proc Natl Acad Sci USA* 98: 373-378.

715 Gao M, Liu J, Bi D, Zhang Z, Cheng F, Chen S, Zhang Y (2008) MEKK1,
716 MKK1/MKK2 and MPK4 function together in a mitogen-activated protein kinase
717 cascade to regulate innate immunity in plants. *Cell Res*. 18: 1190-1198.

718 Haas BJ, Kamoun S, Zody MC et al. (2009) Genome sequence and analysis of the
719 Irish potato famine pathogen *Phytophthora infestans*. *Nature* 461: 393-398.

720 Hashimoto M, Komatsu K, Maejima K, Okano Y, Shiraishi T, Ishikawa K, Takinami Y,
721 Yamaji Y, Namba S (2012) Identification of three MAPKKKs forming a linear
722 signaling pathway leading to programmed cell death in *Nicotiana benthamiana*.
723 *BMC Plant Biol*. 12: 103.

724 Jin H, Axtell MJ, Dahlbeck D, Ekwenna O, Zhang S, Staskawicz B, Baker B (2002)
725 NPK1, an MEKK1-like mitogen-activated protein kinase kinase kinase, regulates
726 innate immunity and development in plants. *Dev Cell* 3: 291-297.

727 Jones J, Dangl J (2006) The plant immune system. *Nature* 444: 323-329.

728 Kamoun S, Furzer O, Jones JD, Judelson HS, Ali GS., et al. (2015) The top 10
729 oomycete pathogens in molecular plant pathology. *Mol Plant Pathol*. 16: 413-434.

730 Kamoun S, van West, PVleeshouwers VG, de Groot KE, Govers F (1998)
731 Resistance of *Nicotiana benthamiana* to *Phytophthora infestans* is mediated by
732 the recognition of the elicitor protein INF1. *Plant Cell* 10: 1413-1426.

733 King SR, McLellan H, Boevink PC, Armstrong MR, Bukharova T, Sukarta O, Win J,
734 Kamoun S, Birch PR, Banfield MJ (2014) *Phytophthora infestans* RXLR effector
735 PexRD2 interacts with host MAPKKKε to suppress plant immune signaling. *Plant*
736 *Cell* 26: 1345-1359.

737 Liu Y, Schiff M, Marathe R, Dinesh-Kumar SP (2002) Tobacco Rar1, EDS1 and

738 NPR1/NIM1 like genes are required for N-mediated resistance to tobacco mosaic
739 virus. *Plant J*. 30: 415-429.

740 MAPK Group (2002) Mitogen-activated protein kinase cascades in plants: a new
741 nomenclature. *Trends Plant Sci*. 7: 301-308.

742 McLellan H, Boevink PC, Armstrong MR, Pritchard L, Gomez S, Morales J, Whisson
743 SC, Beynon JL, Birch PR (2013) An RxLR effector from *Phytophthora infestans*
744 prevents re-localisation of two plant NAC transcription factors from the
745 endoplasmic reticulum to the nucleus. *PLoS Pathog*. 9: e1003670.

746 Melech-Bonfil S, and Sessa G (2010) Tomato MAPKKKε is a positive regulator of
747 cell-death signaling networks associated with plant immunity. *Plant J*. 64:
748 379-391.

749 Moffett P, Farnham G, Peart J, Baulcombe DC (2002) Interaction between domains
750 of a plant NBS-LRR protein in disease resistance-related cell death. *EMBO J*. 21:
751 4511-4519

752 Mukhtar MS, Carvunis A-R, Dreze M, Epple P, Steinbrenner J., et al. (2011)
753 Independently evolved virulence effectors converge onto hubs in a plant immune
754 system network. *Science* 333: 596-600.

755 Murphy F, He Q, Armstrong M, Giuliani LM, Boevink PC, Zhang W, Tian Z, Birch RR,
756 Gilroy EM (2018) Potato MAP3K StVIK is required for *Phytophthora infestans*
757 RXLR Effector Pi17316 to promote disease. *Plant Physiol*. 177(1): 398-410.

758 Pedley KF. Martin GB (2005) Role of mitogen-activated protein kinases in plant
759 immunity. *Curr Opin Plant Biol*. 8: 541-547.

760 Pitzschke A, Schikora A, Hirt H (2009) MAPK cascade signalling networks in plant
761 defence. *Curr Opin Plant Biol*. 12: 421-426.

762 Suarez-Rodriguez MC, Adams-Phillips L, Liu Y, Wang H, Su SH, Jester PJ, Zhang S,
763 Bent AF, Krysan PJ (2007) MEKK1 is required for flg22-induced MPK4 activation
764 in Arabidopsis plants. *Plant Physiol*. 143: 661-669.

765 Sun T, Nitta Y, Zhang Q, Wu D, Tian H, Lee JS, Zhang Y (2018) Antagonistic
766 interactions between two MAP kinase cascades in plant development and
767 immune signaling. *EMBO Reports* 19: e45324.

768 Toruño TY, Stergiopoulos I, Coaker G (2016) Plant-pathogen effectors: cellular
769 probes interfering with plant defenses in special and temporal manners. *Ann Rev*
770 *Phytopathol* 54: 419-441.Wang S, Boevink PC, Welsh L, Zhang R, Whisson SC,
771 Birch PRJ (2017) Delivery of cytoplasmic and apoplastic effectors from
772 *Phytophthora infestans* haustoria by distinct secretion pathways. *New Phytol.* 216:
773 205-215.

774 Wang S, McLellan H, Bukharova T, He Q, Murphy F, et al (2018b) *Phytophthora*
775 *infestans* RXLR effectors act in concert at diverse subcellular localisations to
776 enhance host colonization. *J Exp Bot* 70: 343-356.

777 Wang S, Welsh L, Thorpe P, Whisson SC, Boevink PC, Birch PRJ. (2018a) The
778 *Phytophthora infestans* haustorium is a site for secretion of diverse classes of
779 infection associated proteins. *mBio* 9: e01216-18.

780 Wang X, Boevink P, McLellan H, Armstrong M, Bukharova T, Qin Z, Birch PR (2015)
781 A Host KH RNA-Binding protein is a susceptibility factor targeted by an RXLR
782 effector to promote Late blight disease. *Mol Plant* 8: 1385-1395.

783 Weβling R, Epple P, Altmann S, He Y, Yang L, et al. (2014) Convergent targeting of
784 a common host protein network by pathogen effectors from three kingdoms of life.
785 *Cell Host Microbe* 16: 364-375.

786 Whisson SC, Boevink PC, Moleleki L, Avrova AO, Morales JG, Gilroy EM, Armstrong
787 MR, Grouffaud S, West PV, Chapman S et al. (2007) A translocation signal for
788 delivery of oomycete effector proteins into host plant cells. *Nature* **450**: 115-118.

789 Whisson SC, Boevink PC, Wang S, Birch PR (2016) The cell biology of late blight
790 disease. *Curr Opin Microbiol*. 34: 127-135.

791 Yang L, McLellan H, Naqvi S, He Q, Boevink PC, Armstrong M, Giuliani LM, Zhang

W, Tian Z, Zhan J, Gilroy EM, Birch PR (2016) Potato NPH3/RPT2-Like protein StNRL1, targeted by a *Phytophthora infestans* RXLR effector, is a susceptibility factor. *Plant Physiol*.171: 645-657.

Yin JL, Gu B, Huang GY, Tian Y, Quan JL, Lindqvist-Kreuze H, Shan WX (2017) Conserved RXLR effector genes of *Phytophthora infestans* expressed at the early stage of potato infection are suppressive to host defense. *Front Plant Sci.* 8: 2155.

Zheng X, McLellan H, Fraiture M, Liu X, Boevink PC, Gilroy EM, Ying C, Kandel K, Sessa G, Birch PR, Brunner F (2014) Functionally redundant RXLR effectors from *Phytophthora infestans* act at different steps to suppress early flg22-triggered immunity. *PLoS Pathog.* 10(4): e1004057.

Figure 1

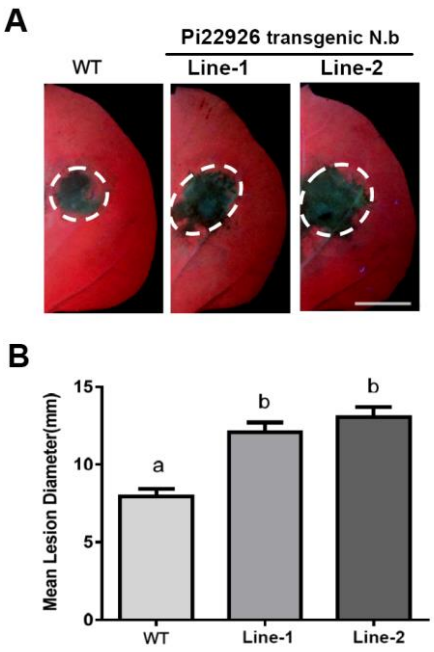

Figure 1. The RXLR effector Pi22926 enhances *P. infestans* colonization of *N. benthamiana* leaves. (A) Representative images taken under UV light at 5 days after inoculation show that transgenic lines overexpressing GFP-Pi22926 enhance pathogen colonization compared to the untransformed *N. benthamiana* control. Scale bar represents 1 cm. (B) Graph shows a significant increase in *P. infestans* lesions in transgenic lines overexpressing GFP-Pi22926 compared to wild type *N. benthamiana* control (ANOVA, $p<0.001$, 3 reps, n=120). Lowercase letters on graphs denote statistically significant groups. Error bars represent ± SE.

Figure 2

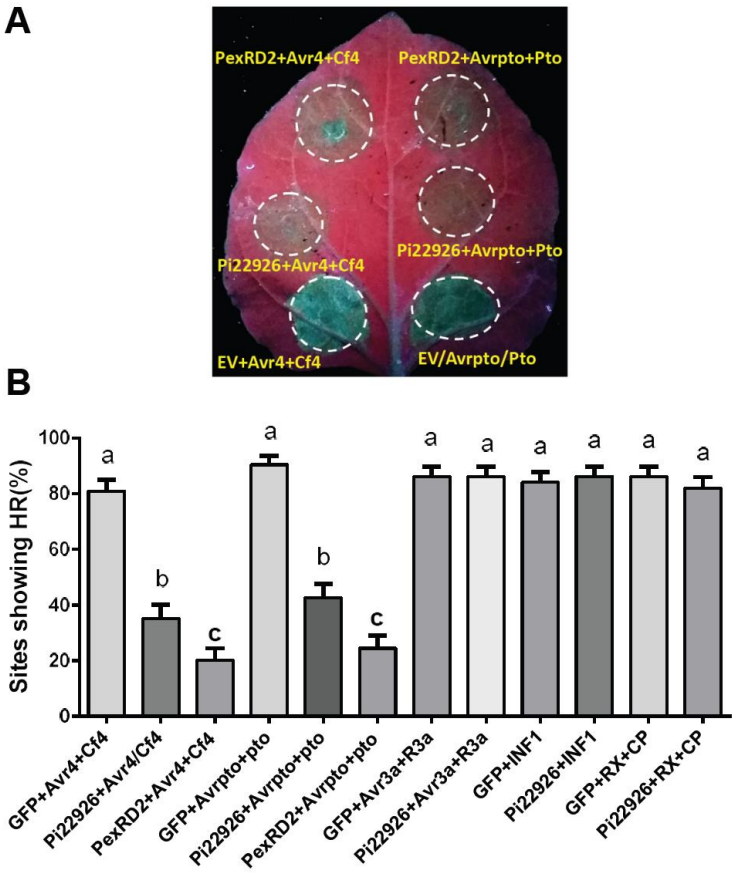

Figure 2. Pi22926 specifically suppresses Avr4/Cf4 and AvrPto/Pto induced cell death. (A) Representative leaf image taken under UV light at 5 days showing Avr4/Cf4 and AvrPto/Pto cell death with EV, Pi22926 and PexRD2 positive control. (B) Graph showing Pi22926 and PexRD2 expression lead to a significant decrease ($p<0.001$, 3 reps, n=94) in cell death percentage trigged by Avr4/Cf4 and AvrPto/Pto. Lowercase letters on graphs denote statistically significant groups by one-way ANOVA, with pairwise comparisons performed with the Holm-Sidak method. Error bars represent ± SE.

Figure 3

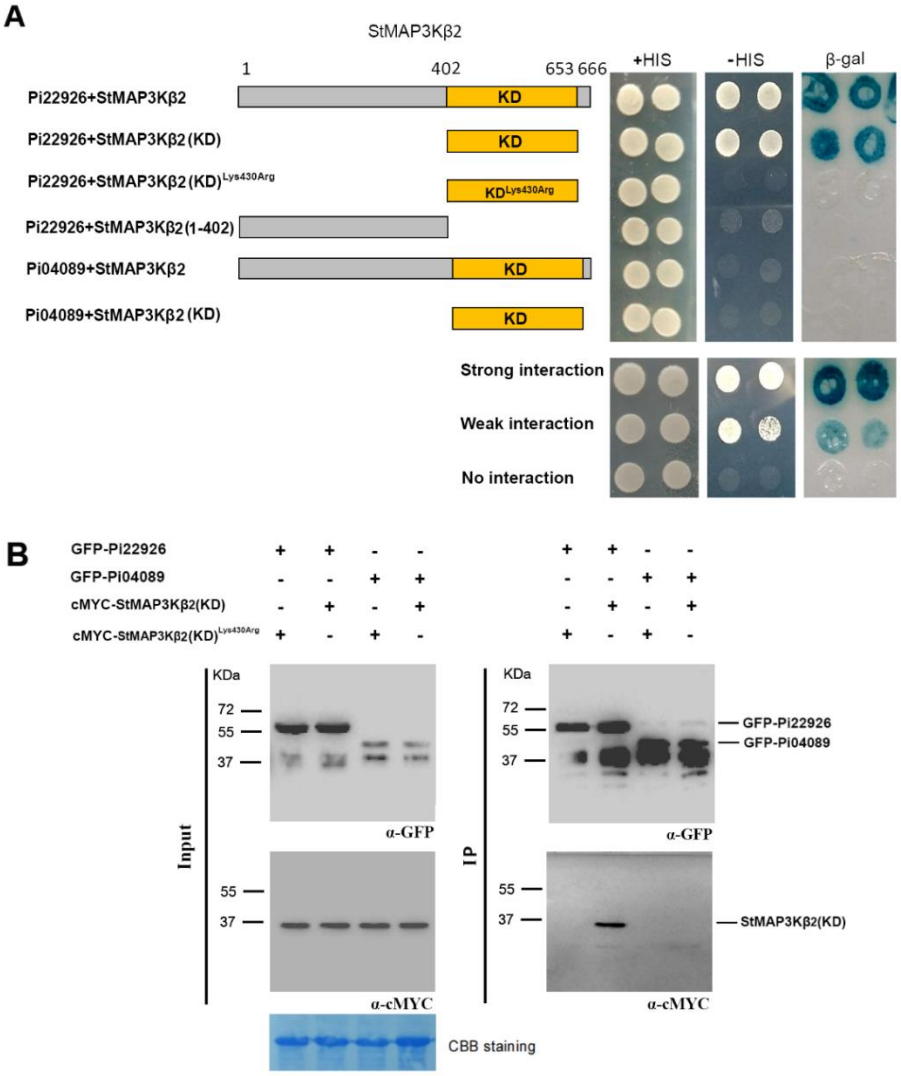

Figure 3. Pi22926 interacts with the kinase domain of StMAP3Kβ2 in Y2H and immunoprecipitation assays. (A) Yeast co-expressing Pi22926 with StMAP3Kβ2 and its kinase domain grow on –histidine (-HIS) medium and had β-galactosidase (β-gal) activity, whereas those co-expressed with the inactive mutant kinase domain StMAP3Kβ2(KD)^{Lys430Arg} or the control Pi04089 did not. (B) Co-immunoprecipitation from leaf extracts using GFP-trap (GFP IP) confirmed that cMyc tagged StMAP3Kβ2 KD specifically interacted with GFP-Pi22926 and not with Pi04089. Expression of constructs is indicated by +. Protein size markers are indicated in KDa, and protein loading is indicated by Coomassie brilliant blue (CBB) staining.

Figure 4

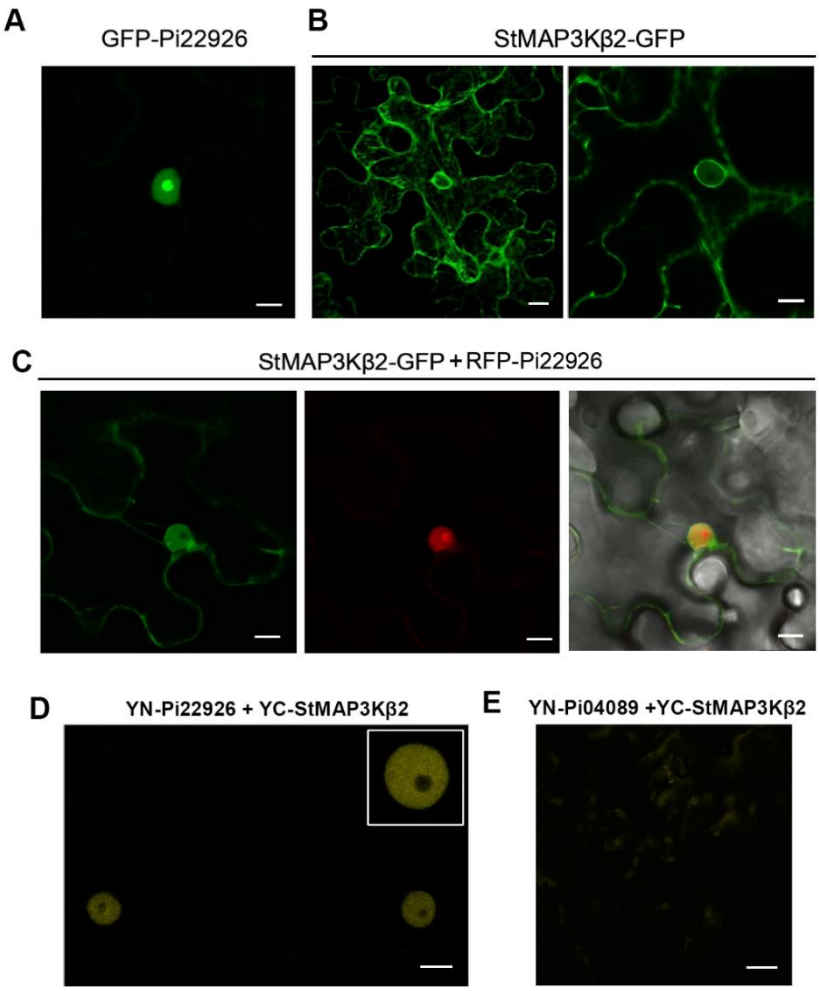

Figure 4. Pi22926 interacts with StMAP3Kβ2 in nucleoplasm. (A) Confocal images show that GFP-Pi22926 is localized in the nucleoplasm and nucleolus. (B) StMAP3Kβ2-GFP is localized in the cytoplasm and nucleoplasm. For images of StMAP3Kβ2-GFP, the left one is a Z-stack, whereas the right one with higher magnification is a single optical section from the stack. (C) Images show transient co-expression of StMAP3Kβ2-GFP with RFP-Pi22926. (D) Images show transient co-expression of YC-StMAP3Kβ2 with YN-Pi22926. Inset image is a nucleus at higher magnification. (E) Images show transient co-expression of YC-StMAP3Kβ2 with YN-Pi04089. Scale bars represent 10 μm. OD_{600} of Agrobacteria suspension for GFP and RFP constructs is 0.1 and 0.03 for split YFP.

Figure 5

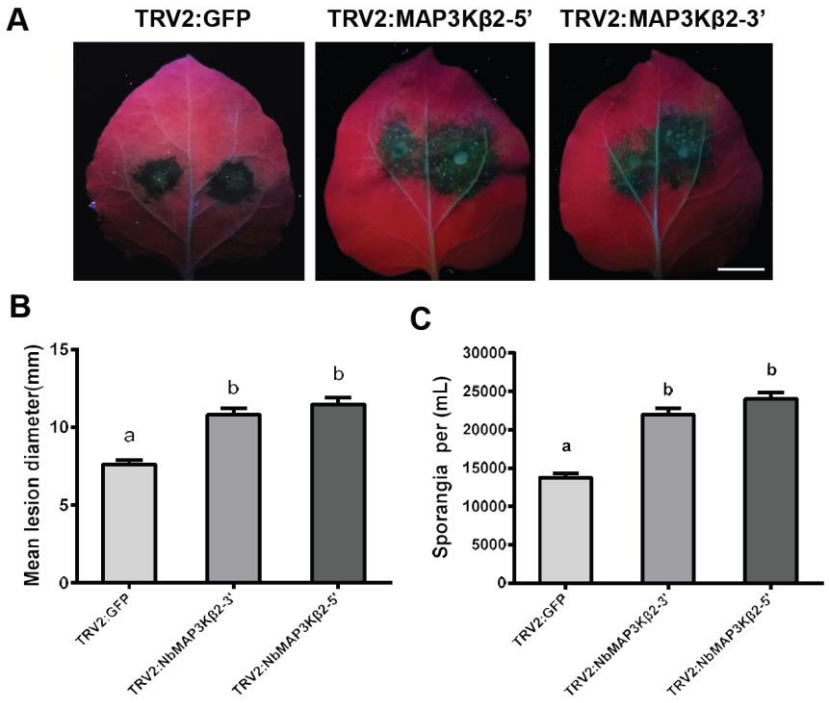

Figure 5. Silencing of *NbMAP3Kβ2* enhances *P. infestans* leaf colonization. (A) Images taken at 7 days after sporangia inoculation indicate more pathogen colonization on TRV:NbMAP3Kβ2 plants compared to the TRV:GFP control. Scale bar represents 1 cm. (B) Graph shows a significant increase (ANOVA, $p<0.001$, 3 reps, n=120) in *P. infestans* lesion diameter in plants expressing TRV:NbMAP3Kβ2-3' and TRV:NbMAP3Kβ2-5', compared with a TRV-GFP control. (C) Graph shows an increase in the average numbers of sporangia mL^{-1} collected from infected leaves expressing TRV:NbMAP3Kβ2-3' and TRV:NbMAP3Kβ2-5', compared with a TRV:GFP control (ANOVA, $p<0.001$, 3 reps, n=120). Lowercase letters on graphs denote statistically significant groups. Error bars represent ± SE.

Figure 6

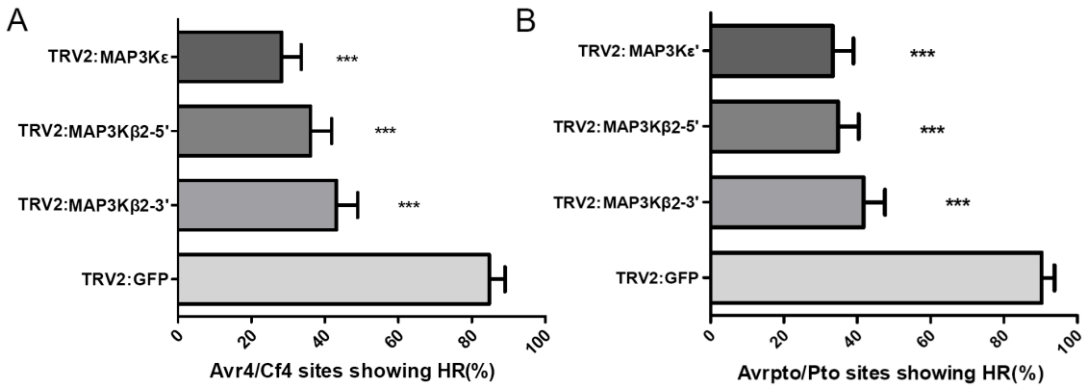

Figure 6. Cell death induced by Avr4/Cf4 and Avrpto/Pto is dependent on MAP3Kε and NbMAP3Kβ2. (A) Graph showing a significant suppression of cell death (ANOVA, p<0.001, 3 reps, n=72) induced by Avr4/Cf4 in *NbMAP3Kβ2* silenced plants, and in positive control *NbMAP3Kε* silenced plants, compared to TRV2:GFP control. (B) Graph showing a significant decrease of cell death (ANOVA, p<0.001, 3 reps, n=72) triggered by Avrpto/Pto in *NbMAP3Kβ2* silenced plants, and positive control *NbMAP3Kε* silenced plants, compared to TRV2:GFP control. Error bars represent ± SE. Cell death numbers were counted at 6 days. Stars indicate significant difference to the TRV:GFP control.

Figure 7

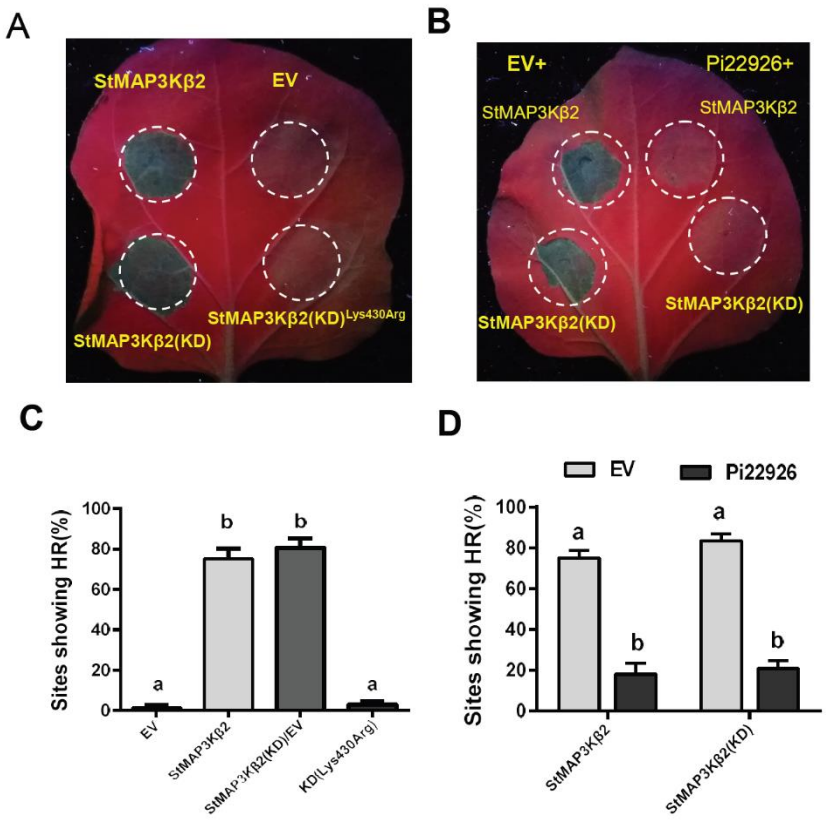

Figure 7. Overexpression of StMAP3Kβ2 or its kinase domain induces cell death that is suppressed by Pi22926. (A) Images taken under UV light at 7 days after inoculation showing that transient overexpression of StMAP3Kβ2 and its kinase domain induce cell death in *N. benthamiana* whereas no cell death was triggered by the expression of the inactive mutant StMAP3Kβ2 (KD)^{Lys430Arg} or the empty vector control. (B) The cell death trigged by StMAP3Kβ2 and its active kinase domain is suppressed by co-expression with Pi22926, but not EV control. Images taken under UV light at 7 days. (C) Graph shows a significant increase in percentage of cell death compared to EV control and inactive mutant KD (ANOVA, $p<0.001$, 3 reps, n=72). (D) Graph shows that transient overexpression of Pi22926 can significantly suppress the cell death (ANOVA, $p<0.001$, 3 reps, n=72) induced by StMAP3Kβ2 and its active KD compared to EV control. Lowercase letters on graphs denote statistically significant groups. Error bars represent ± SE.

Figure 8

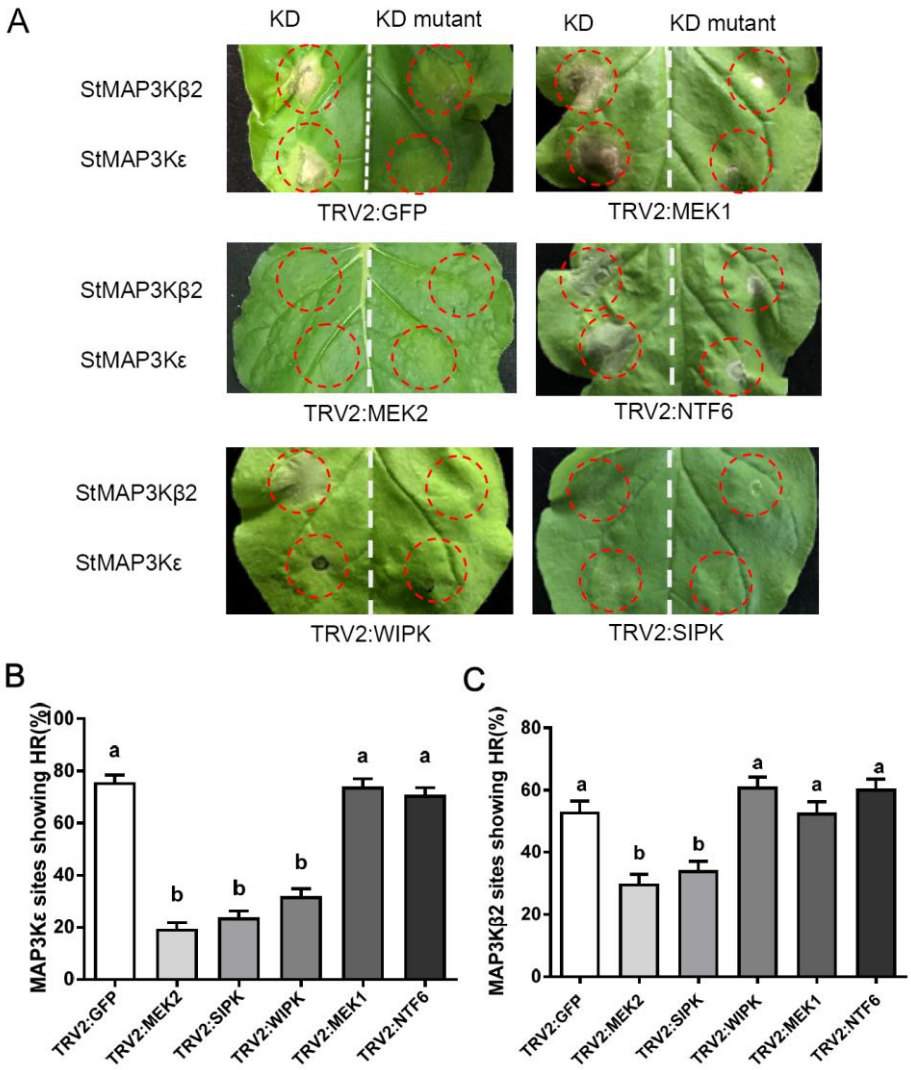

Figure 8. MEK2 and SIPK act downstream of StMAP3Kβ2. (A) *N. benthamiana* plants were infected with TRV:GFP only or were silenced for the indicated MAP2Ks (*MEK1* or *MEK2*) and MAPK (*SIPK, WIPK* or *NTF6*) genes. StMAP3Kβ2 kinase domain (KD) or inactive (KD mutant) were expressed in the leaves to measure cell death. Photos were taken under UV light at 7 days. (B) and (C) Graph showing a significant suppression of cell death trigged by StMAP3Kε(KD) or StMAP3Kβ2(KD) in TRV2:MEK2 and TRV2:SIPK plants compared to the TRV2:GFP control (ANOVA, $p<0.001$, 3 reps, $n\geq155$). Error bars represent ± SE.

Figure 9

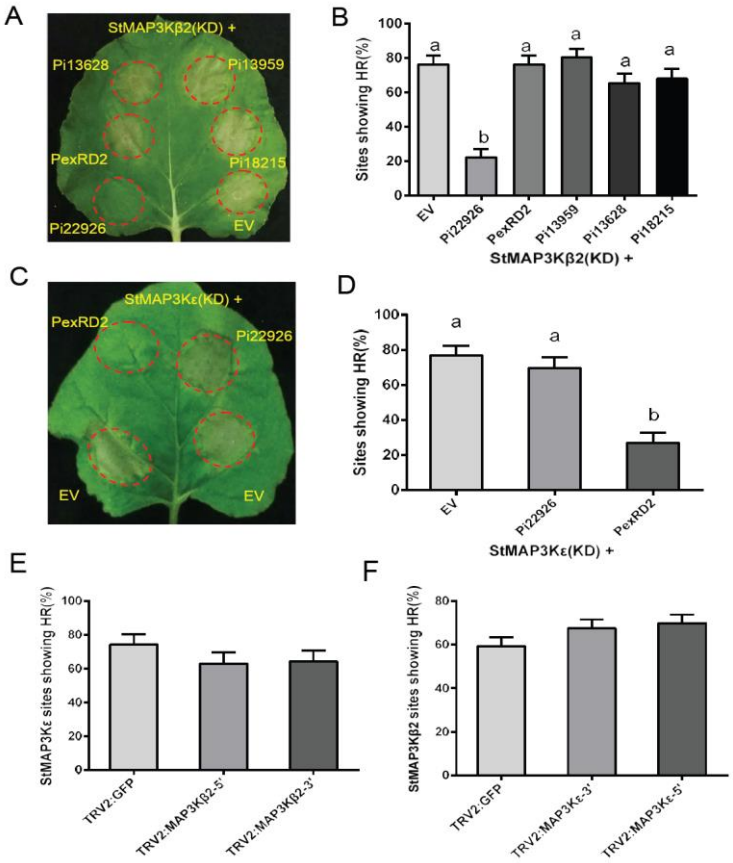

Figure 9. Pi22926 suppresses cell death trigged by StMAP3Kβ2 whereas PexRD2 suppresses StMAP3Kε-induced cell death. (A) and (C) Images showing StMAP3Kβ2 (KD) and StMAP3Kε(KD) cell death at 7 days, following co-expression with indicated effectors. (B) and (D) Graphs showing percentage of inoculation sites developing cell death at 7 days after co-expression of StMAP3Kβ2(KD) or StMAP3Kε(KD) with indicated effectors. A significant decrease of cell death percentage was observed when Pi22926 was co-expressed with StMAP3Kβ2(KD) or when PexRD2 was co-expressed with StMAP3Kε(KD), compared to co-expression with other effectors and the EV control (ANOVA, $p<0.001$, 4 reps, $n=73$). Lowercase letters on graphs denote statistically significant groups. Error bars represent ± SE. (E) Graph shows no significant decrease in mean percentage of cell death induced by StMAP3Kε in TRV2:NbMAP3Kβ2-3' and TRV2:NbMAP3Kβ2-5' plants compared to the TRV2-GFP control (7 days) (ANOVA, $p<0.001$, 4 reps, $n=92$) and (F) Graph shows that VIGS of MAP3Kε by TRV2:NbMAP3Kε-3' and TRV2-NbMAP3Kε-5' had no significant effect on StMAP3Kβ2-induced cell death compared to the TRV:GFP control (7 days). (ANOVA, $p<0.001$, 4 reps, $n=132$). Error bars represent ± SE.

Figure 10

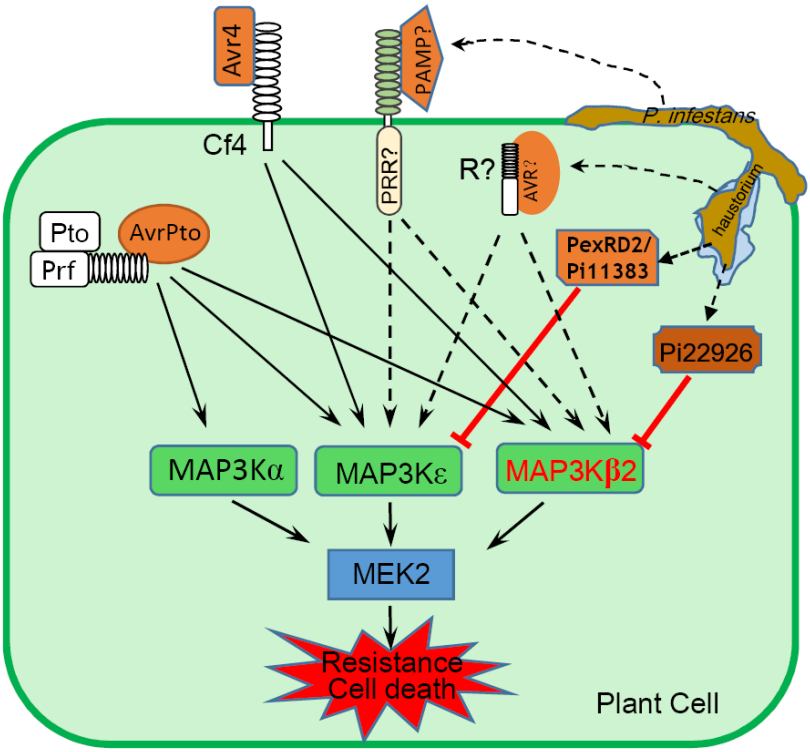

Figure 10. Model of how PexRD2 and Pi22926 suppress two parallel MAPK signalling pathways triggered by Avr4/Cf4 or AvrPto/Pto. Schematic diagram illustrating *P. infestans* delivering PexRD2 and Pi22926 inside the host cell during infection. The cell death following recognition of the *C. fulvum* effector Avr4 by Cf4 and the *P. syringe* effector AvrPto mediated by Pto/Prf are dependent on MAPKKKε or MAP3Kβ2 is suppressed respectively by the presence of PexRD2 or Pi22926. PexRD2 or Pi22926 specifically interact with MAPKKKε or MAP3Kβ2 respectively. *In planta*, MAPKKKε and MAP3Kβ2 confer enhanced resistance against *P. infestans* likely due to recognition of an unidentified PAMP by a PRR or recognition of an effector/avirulence protein (AVR) by an R protein as proposed by King et al. (2014).

Parsed Citations

Ah Fong AMV, Kim KS, Judelson HS (2017) RNA-seq of life stages of the oomycete Phytophthora infestans reveals dynamic changes in metabolic, signal transduction, and pathogenesis genes and a major role for calcium signaling in development. BMC Genomics 18: 198.
Pubmed: Author and Title
Google Scholar: Author Only Title Only Author and Title

Anderson RG, Deb D, Fedkenheuer K, McDowell JM (2015). Recent Progress in RXLR Effector Research. Mol Plant Microbe Interact 28, 1063-1072.
Pubmed: Author and Title
Google Scholar: Author Only Title Only Author and Title

Armstrong MR, Whisson SC, Pritchard L, Bos JI, Venter E, Avrova AO, Rehmany AP, Böhme U, Brooks K, Cherevach I, Hamlin N, White B, Fraser A, Lord A, Quail MA, Churcher C, Hall N, Berriman M, Huang S, Kamoun S, Beynon JL, Birch PR (2005) An ancestral oomycete locus contains late blight avirulence gene Avr3a, encoding a protein that is recognized in the host cytoplasm. Proc Natl Acad Sci USA 102: 7766-7771.
Pubmed: Author and Title
Google Scholar: Author Only Title Only Author and Title

Asai S, Ohta K, Yoshioka H (2008) MAPK signaling regulates nitric oxide and NADPH oxidase-dependent oxidative bursts in Nicotiana benthamiana. Plant Cell 20: 1390-406.
Pubmed: Author and Title
Google Scholar: Author Only Title Only Author and Title

Bi G, Zhou JM (2017) MAP kinase signaling pathways: a hub of plant-microbe interactions. Cell Host and Microbe 21: 270-273.
Pubmed: Author and Title
Google Scholar: Author Only Title Only Author and Title

Bi G, Zhou Z, Wang W, Li L, Rao S, Wu Y, Zhang X, Menke FLH, Chen S, Zhou J-M (2018) Receptor-like cytoplasmic kinases directly link pattern recognition receptors to the activation of mitogen-activated protein kinase cascades. Plant Cell 30: 1543-1561.
Pubmed: Author and Title
Google Scholar: Author Only Title Only Author and Title

Block A, Alfano JR (2011) Plant targets for Pseudomonas syringae type III effectors: virulence targets or guarded decoys? Curr Opin Microbiol. 14: 39-46.
Pubmed: Author and Title
Google Scholar: Author Only Title Only Author and Title

Bos JI, Armstrong MR, Gilroy EM, Boevink PC, Hein I, Taylor RM, Tian Z, Engelhardt S, Vetukuri RR, Harrower B, Dixelius C, Bryan G, Sadanandom A, Whisson SC, Kamoun S, Birch PR (2010) Phytophthora infestans effector AVR3a is essential for virulence and manipulates plant immunity by stabilizing host E3 ligase CMPG1. Proc Natl Acad Sci USA 107: 9909-9914.
Pubmed: Author and Title
Google Scholar: Author Only Title Only Author and Title

Chisholm ST, Coaker G, Day B, Staskawicz BJ (2006) Host–microbe interactions: shaping the evolution of the plant immune response. Cell 124: 803-814.
Pubmed: Author and Title
Google Scholar: Author Only Title Only Author and Title

Colcombet J, Hirt H (2008) Arabidopsis MAPKs: a complex signalling network involved in multiple biological processes. Biochemical J. 413: 217-226.
Pubmed: Author and Title
Google Scholar: Author Only Title Only Author and Title

Cooke DE, Cano LM, Raffaele S, Bain RA, Cooke LR, Etherington GJ, Deahl KL, Farrer RA, Gilroy EM, Goss EM, Grünwald NJ, Hein I, MacLean D, McNicol JW, Randall E, Oliva RF, Pel MA, Shaw DS, Squires JN, Taylor MC, Vleeshouwers VG, Birch PR, Lees AK, Kamoun S (2012) Genome analyses of an aggressive and invasive lineage of the Irish potato famine pathogen. PLoS Pathog. 8: e1002940.
Pubmed: Author and Title
Google Scholar: Author Only Title Only Author and Title

Couto D, Zipfel C (2016) Regulation of pattern recognition receptor signalling in plants. Nat Rev Immunol. 16: 537-552.
Pubmed: Author and Title
Google Scholar: Author Only Title Only Author and Title

Cui H, Wang Y, Xue L, Chu J, Yan C, Fu J, Chen M, Innes RW, Zhou JM (2010) Pseudomonas syringae effector protein AvrB perturbs Arabidopsis hormone signalling by activating MAP kinase 4. Cell Host Microbe 7: 164-175.
Pubmed: Author and Title
Google Scholar: Author Only Title Only Author and Title

del Pozo O, Pedley KF, Martin GB (2004) MAPKKKalpha is a positive regulator of cell death associated with both plant immunity and disease. EMBO J. 23: 3072-3082.
Pubmed: Author and Title
Google Scholar: Author Only Title Only Author and Title

Deslandes L, Rivas S (2012) Catch me if you can: bacterial effectors and plant targets. Trends Plant Sci. 17: 644-655.
Pubmed: Author and Title
Google Scholar: Author Only Title Only Author and Title

Dodds PN, Rathjen JP (2010) Plant immunity: Towards an integrated view of plant-pathogen interactions. Nat Rev Genet. 11: 539-548.
Pubmed: Author and Title
Google Scholar: Author Only Title Only Author and Title

Dou D, Kale SD, Wang X, Jiang RH, Bruce NA, Arredondo FD, Zhang X, Tyler BM. (2008) RXLR-mediated entry of Phytophthora sojae effector Avr1b into soybean cells does not require pathogen-encoded machinery. Plant Cell 20: 1930-1947.
Pubmed: Author and Title
Google Scholar: Author Only Title Only Author and Title

Dou D, Zhou JM (2012) Phytopathogen effectors subverting host immunity: different foes, similar battleground. Cell Host Microbe 12: 484-495.
Pubmed: Author and Title
Google Scholar: Author Only Title Only Author and Title

Ekengren SK, Liu Y, Schiff M, Dinesh-Kumar SP, Martin GB (2003) Two MAPK cascades, NPR1, and TGA transcription factors play a role in Pto-mediated disease resistance in tomato. Plant J. 36: 905-917.
Pubmed: Author and Title
Google Scholar: Author Only Title Only Author and Title

Frye CA, Tang D, Innes RW (2001) Negative regulation of defense responses in plants by a conserved MAPKK kinase. Proc Natl Acad Sci USA 98: 373-378.
Pubmed: Author and Title
Google Scholar: Author Only Title Only Author and Title

Gao M, Liu J, Bi D, Zhang Z, Cheng F, Chen S, Zhang Y (2008) MEKK1, MKK1/MKK2 and MPK4 function together in a mitogen-activated protein kinase cascade to regulate innate immunity in plants. Cell Res. 18: 1190-1198.
Pubmed: Author and Title
Google Scholar: Author Only Title Only Author and Title

Haas BJ, Kamoun S, Zody MC et al. (2009) Genome sequence and analysis of the Irish potato famine pathogen Phytophthora infestans. Nature 461: 393-398.
Pubmed: Author and Title
Google Scholar: Author Only Title Only Author and Title

Hashimoto M, Komatsu K, Maejima K, Okano Y, Shiraishi T, Ishikawa K, Takinami Y, Yamaji Y, Namba S (2012) Identification of three MAPKKKs forming a linear signaling pathway leading to programmed cell death in Nicotiana benthamiana. BMC Plant Biol. 12: 103.
Pubmed: Author and Title
Google Scholar: Author Only Title Only Author and Title

Jin H, Axtell MJ, Dahlbeck D, Ekwenna O, Zhang S, Staskawicz B, Baker B (2002) NPK1, an MEKK1-like mitogen-activated protein kinase kinase kinase, regulates innate immunity and development in plants. Dev Cell 3: 291-297.
Pubmed: Author and Title
Google Scholar: Author Only Title Only Author and Title

Jones J, Dangl J (2006) The plant immune system. Nature 444: 323-329.
Pubmed: Author and Title
Google Scholar: Author Only Title Only Author and Title

Kamoun S, Furzer O, Jones JD, Judelson HS, Ali GS., et al. (2015) The top 10 oomycete pathogens in molecular plant pathology. Mol Plant Pathol. 16: 413-434.
Pubmed: Author and Title
Google Scholar: Author Only Title Only Author and Title

Kamoun S, van West, PVleeshouwers VG, de Groot KE, Govers F (1998) Resistance of Nicotiana benthamiana to Phytophthora infestans is mediated by the recognition of the elicitor protein INF1. Plant Cell 10: 1413-1426.
Pubmed: Author and Title
Google Scholar: Author Only Title Only Author and Title

King SR, McLellan H, Boevink PC, Armstrong MR, Bukharova T, Sukarta O, Win J, Kamoun S, Birch PR, Banfield MJ (2014) Phytophthora infestans RXLR effector PexRD2 interacts with host MAPKKKε to suppress plant immune signaling. Plant Cell 26: 1345-1359.
Pubmed: Author and Title
Google Scholar: Author Only Title Only Author and Title

Liu Y, Schiff M, Marathe R, Dinesh-Kumar SP (2002) Tobacco Rar1, EDS1 and NPR1/NIM1 like genes are required for N-mediated resistance to tobacco mosaic virus. Plant J. 30: 415-429.
Pubmed: Author and Title
Google Scholar: Author Only Title Only Author and Title

MAPK Group (2002) Mitogen-activated protein kinase cascades in plants: a new nomenclature. Trends Plant Sci. 7: 301-308.
Pubmed: Author and Title

Google Scholar: Author Only Title Only Author and Title

McLellan H, Boevink PC, Armstrong MR, Pritchard L, Gomez S, Morales J, Whisson SC, Beynon JL, Birch PR (2013) An RxLR effector from Phytophthora infestans prevents re-localisation of two plant NAC transcription factors from the endoplasmic reticulum to the nucleus. PLoS Pathog. 9: e1003670.
Pubmed: Author and Title
Google Scholar: Author Only Title Only Author and Title

Melech-Bonfil S, and Sessa G (2010) Tomato MAPKKKε is a positive regulator of cell-death signaling networks associated with plant immunity. Plant J. 64: 379-391.
Pubmed: Author and Title
Google Scholar: Author Only Title Only Author and Title

Moffett P, Farnham G, Peart J, Baulcombe DC (2002) Interaction between domains of a plant NBS-LRR protein in disease resistance-related cell death. EMBO J. 21: 4511-4519
Pubmed: Author and Title
Google Scholar: Author Only Title Only Author and Title

Mukhtar MS, Carvunis A-R, Dreze M, Epple P, Steinbrenner J., et al. (2011) Independently evolved virulence effectors converge onto hubs in a plant immune system network. Science 333: 596-600.
Pubmed: Author and Title
Google Scholar: Author Only Title Only Author and Title

Murphy F, He Q, Armstrong M, Giuliani LM, Boevink PC, Zhang W, Tian Z, Birch RR, Gilroy EM (2018) Potato MAP3K StVIK is required for Phytophthora infestans RXLR Effector Pi17316 to promote disease. Plant Physiol. 177(1): 398-410.
Pubmed: Author and Title
Google Scholar: Author Only Title Only Author and Title

Pedley KF. Martin GB (2005) Role of mitogen-activated protein kinases in plant immunity. Curr Opin Plant Biol. 8: 541-547.
Pubmed: Author and Title
Google Scholar: Author Only Title Only Author and Title

Pitzschke A, Schikora A, Hirt H (2009) MAPK cascade signalling networks in plant defence. Curr Opin Plant Biol. 12: 421-426.
Pubmed: Author and Title
Google Scholar: Author Only Title Only Author and Title

Suarez-Rodriguez MC, Adams-Phillips L, Liu Y, Wang H, Su SH, Jester PJ, Zhang S, Bent AF, Krysan PJ (2007) MEKK1 is required for flg22-induced MPK4 activation in Arabidopsis plants. Plant Physiol. 143: 661-669.
Pubmed: Author and Title
Google Scholar: Author Only Title Only Author and Title

Sun T, Nitta Y, Zhang Q, Wu D, Tian H, Lee JS, Zhang Y (2018) Antagonistic interactions between two MAP kinase cascades in plant development and immune signaling. EMBO Reports 19: e45324.
Pubmed: Author and Title
Google Scholar: Author Only Title Only Author and Title

Toruño TY, Stergiopoulos I, Coaker G (2016) Plant-pathogen effectors: cellular probes interfering with plant defenses in special and temporal manners. Ann Rev Phytopathol 54: 419-441.Wang S, Boevink PC, Welsh L, Zhang R, Whisson SC, Birch PRJ (2017) Delivery of cytoplasmic and apoplastic effectors from Phytophthora infestans haustoria by distinct secretion pathways. New Phytol. 216: 205-215.
Pubmed: Author and Title
Google Scholar: Author Only Title Only Author and Title

Wang S, McLellan H, Bukharova T, He Q, Murphy F, et al (2018b) Phytophthora infestans RXLR effectors act in concert at diverse subcellular localisations to enhance host colonization. J Exp Bot 70: 343-356.
Pubmed: Author and Title
Google Scholar: Author Only Title Only Author and Title

Wang S, Welsh L, Thorpe P, Whisson SC, Boevink PC, Birch PRJ. (2018a) The Phytophthora infestans haustorium is a site for secretion of diverse classes of infection associated proteins. mBio 9: e01216-18.
Pubmed: Author and Title
Google Scholar: Author Only Title Only Author and Title

Wang X, Boevink P, McLellan H, Armstrong M, Bukharova T, Qin Z, Birch PR (2015) A Host KH RNA-Binding protein is a susceptibility factor targeted by an RXLR effector to promote Late blight disease. Mol Plant 8: 1385-1395.
Pubmed: Author and Title
Google Scholar: Author Only Title Only Author and Title

Weβling R, Epple P, Altmann S, He Y, Yang L, et al. (2014) Convergent targeting of a common host protein network by pathogen effectors from three kingdoms of life. Cell Host Microbe 16: 364-375.
Pubmed: Author and Title
Google Scholar: Author Only Title Only Author and Title

Whisson SC, Boevink PC, Moleleki L, Avrova AO, Morales JG, Gilroy EM, Armstrong MR, Grouffaud S, West PV, Chapman S et al. (2007) A translocation signal for delivery of oomycete effector proteins into host plant cells. Nature 450: 115-118.
Pubmed: Author and Title

Google Scholar: Author Only Title Only Author and Title

Whisson SC, Boevink PC, Wang S, Birch PR (2016) The cell biology of late blight disease. Curr Opin Microbiol. 34: 127-135.
Pubmed: Author and Title
Google Scholar: Author Only Title Only Author and Title

Yang L, McLellan H, Naqvi S, He Q, Boevink PC, Armstrong M, Giuliani LM, Zhang W, Tian Z, Zhan J, Gilroy EM, Birch PR (2016) Potato NPH3/RPT2-Like protein StNRL1, targeted by a Phytophthora infestans RXLR effector, is a susceptibility factor. Plant Physiol.171: 645-657.
Pubmed: Author and Title
Google Scholar: Author Only Title Only Author and Title

Yin JL, Gu B, Huang GY, Tian Y, Quan JL, Lindqvist-Kreuze H, Shan WX (2017) Conserved RXLR effector genes of Phytophthora infestans expressed at the early stage of potato infection are suppressive to host defense. Front Plant Sci. 8: 2155.
Pubmed: Author and Title
Google Scholar: Author Only Title Only Author and Title

Zheng X, McLellan H, Fraiture M, Liu X, Boevink PC, Gilroy EM, Ying C, Kandel K, Sessa G, Birch PR, Brunner F (2014) Functionally redundant RXLR effectors from Phytophthora infestans act at different steps to suppress early flg22-triggered immunity. PLoS Pathog. 10(4): e1004057.
Pubmed: Author and Title
Google Scholar: Author Only Title Only Author and Title